Applied Clay Science 181 (2019) 105209

Contents lists available at ScienceDirect

Applied Clay Science

journal homepage: www.elsevier.com/locate/clay

Research Paper

The role of geological origin of smectites and of their physico-chemical properties on aflatoxin adsorption

Vito D'Ascanio[a], Donato Greco[a], Elena Menicagli[b], Elisa Santovito[a], Lucia Catucci[c], Antonio F. Logrieco[a], Giuseppina Avantaggiato[a,*]

[a] Istituto di Scienze delle Produzioni Alimentari, Consiglio Nazionale delle Ricerche (CNR-ISPA), Bari, Italy
[b] Laviosa Chimica Mineraria SpA, Livorno, Italy
[c] Dipartimento di Chimica, Università degli Studi di Bari Aldo Moro, Bari, Italy

ARTICLE INFO

Keywords:
Aflatoxins
Smectites
Sedimentary bentonites
Hydrothermal bentonites
Adsorption
Desorption

ABSTRACT

Since 2013, bentonite in the form of dioctahedral smectite is an additive authorised in the EU as a substance for the reduction of the contamination of feed by aflatoxins. Several studies indicate a big difference in the effectiveness of smectites in sequestering aflatoxins. A clear correlation between mineralogical and physico-chemical properties of smectites and aflatoxin adsorption has not been well established. In the effort to identify the most critical mineralogical, chemical, and physical properties that affect aflatoxin adsorption by smectites, 29 samples of bentonites obtained from different sources around the world were evaluated. "As received" samples were divided into two main groups, i.e. hydrothermal (n = 14) and sedimentary (n = 15) bentonites depending on their geological origin. The characterization studies showed that all samples contained dioctahedral smectite as major mineral; a moderate CEC value (60-116 cmol/kg); the presence of iron; a small organic matter content; a near-neutral pH; and a fine and uniform particle size (< 45μm). They differed substantially in their sodium, calcium and magnesium contents, and in the swelling properties depending on the geological origin. Several *in vitro* adsorption studies showed that they also differed in a significant manner in adsorbing aflatoxin B_1 (AFB_1). A correlation between geological origin and AFB_1 adsorption capacity was found ($p < 0.001$), being sedimentary smectites significantly more effective than hydrothermal ones in adsorbing the toxin at different pH values. The extent of AFB_1 adsorption by all samples was negatively and linearly correlated to the extent of desorption, and sedimentary smectites were significantly more effective than hydrothermal smectites in keeping bound the adsorbed fraction of the toxin ($p < 0.001$). In addition, correlation studies using the Pearson statistical method showed a significant relationship among some physico-chemical properties of smectites and the amounts of adsorbed toxin. In particular, AFB_1 adsorption by smectites correlated positively with sodium content and swell index, but negatively with d001-value, magnesium and calcium contents. In conclusion, it seems that the geological origin of smectite is a useful guide for the selection of bentonites for AFB_1 detoxification. Sedimentary bentonites containing sodium/swelling-smectite should be preferred to hydrothermal samples as potential aflatoxin binders. Taking into account the geographical origin of our samples, this approach should be applicable to bentonites worldwide.

1. Introduction

Bentonites are formed by highly colloidal and plastic clays composed mainly of montmorillonite, a clay mineral of the smectite group (Phillips et al., 1995; WHO, 2005; Bergaya and Lagaly, 2013). Hundreds of uses reveal the utility of clays in very different fields (Carretero and Lagaly, 2007). Bentonites are broadly distributed around the world, but approximately 90% of the world's bentonite production is concentrated in 22 countries (WHO, 2005). They form mainly from alteration of pyroclastic and/or volcaniclastic rocks (Christidis and Huff, 2009). Extensive deposits, linked to large eruptions, have formed repeatedly in the past. There are three main mechanisms of formation of bentonites with economic importance: (1) in situ diagenetic alteration of volcanic glass; (2) hydrothermal alteration of volcanic glass and (3) formation of Mg-smectite-rich sediments in inland and saline alkaline lakes (Galan and Castillo, 1984). Bentonite composition is partly controlled by parent rock chemistry and is affected by a complex interplay of different factors including temperature, fluid chemistry,

* Corresponding author.
E-mail address: giuseppina.avantaggiato@ispa.cnr.it (G. Avantaggiato).

https://doi.org/10.1016/j.clay.2019.105209
Received 5 April 2019; Received in revised form 8 June 2019; Accepted 7 July 2019
Available online 13 July 2019

reaction time, fluid/rock ratio and probably the composition of the precursor materials (Altaner and Ylagan, 1997; Sinha and Raymahashay, 2004; Miyoshi et al., 2013). Recent studies have shown that bentonite deposits may display cryptic variations in layer charge - i.e. the variations are not visible at the macroscopic scale - and these correlate with physical properties (Christidis and Huff, 2009). This explain why bentonites with the same chemical constituents may have very different properties and minerals with identical properties may have very different chemical constituents. It all depends on how the atoms are arranged. These "cryptic variations" in physico-chemical properties of bentonites may be a cause of the different behavior of bentonites in adsorbing aflatoxins.

Aflatoxins are secondary metabolites of moulds and are the strongest animal carcinogen (Avantaggiato and Visconti, 2009; JECFA, 2018). Aflatoxin B_1 (AFB_1) is the most toxic to humans and animals. Its metabolite aflatoxin M_1 appears in milk and milk products as a direct result of the animal ingesting feed contaminated with AFB_1 (EFSA, 2004). The use of clay minerals, mainly montmorillonite, to alleviate aflatoxin toxicity was started in the late 1970s (Masimango et al., 1978, 1979). Plentiful literature is available on this issue, primarily in the field of *in vitro* aqueous experiments (Phillips et al., 1995; Ramos and Hernández, 1996; Charturvedi et al., 2002; Phillips et al., 2008; Li et al., 2018) and animal feed trials (Phillips et al., 1988; Marquez and Hernandez, 1995; Nahm, 1995; Desheng et al., 2005; Magnoli et al., 2008; Vila-Donat et al., 2018). A further step was the use of smectite in human nutrition; in particular, the effectiveness of a smectite as an agent for decreasing biomarkers of aflatoxin exposure was found (Afriyie-Gyawu et al., 2008a; Phillips et al., 2008; Wang et al., 2008), and its safety for humans after ingestion was studied (Afriyie-Gyawu et al., 2008b; Wang et al., 2005). In Europe, bentonite is authorised as a feed additive under the category of technological additives and the functional groups: *i*) 'binder', 'substance for control of radionuclide contamination' and 'anticaking agent' (1m558*i*), for all animal species; and *ii*) 'substance for reduction of the contamination of feed by mycotoxins (AFB_1)' for ruminants, poultry and pigs (1m558) (EU, 2013). The authorisation of bentonite as food additive expired on the 31st of May 2013 (EU, 2012).

Several *in vitro* studies indicate a big difference in the effectiveness of bentonites in sequestering AFB_1. These studies suggest that AFB_1 adsorption efficacy of a bentonite may depend on physical, chemical and mineralogical properties of the smectite, such as its content in the clay, cation exchange capacity (CEC), hydrated radius of the interlayer cation, particle size distribution, specific surface area, Fourier Transform Infrared (FTIR) evidence of iron and/or magnesium in the smectite structure, pH, and organic carbon content (Phillips et al., 1995; Grant and Phillips, 1998; Barrientos-Velázquez et al., 2016). Some authors tried to explain which of these properties is involved in the AFB_1 adsorption process. Phillips et al. (1995) suggested a relationship between AFB_1 adsorption and surface area of the smectite. Tenorio Arvide et al. (2008) observed that the structural composition of the octahedral sheet in smectites affected their aflatoxin adsorption capacity: the smectites with certain amount of structural iron and magnesium octahedral substitutions had higher aflatoxin adsorption capacities than the smectites with less octahedral substitutions for aluminum, which was confirmed by Dixon et al. (2008). In addition, latter Authors stated that good AFB_1 binding bentonites should be dominantly smectite clays with a CEC recommended at 70 cmol/kg; they should have a particle size set at 35 to 60 Δμ; a pH between 5 and 9; and a low carbon content (Dixon et al., 2008). Further studies demonstrated that high-charge density smectites had low adsorption and poor affinity for AFB_1 (Jaynes and Zartman, 2011; Deng et al., 2012; Barrientos-Velázquez et al., 2016). Saturation of smectite with divalent cations enhanced adsorption capacity and affinity for aflatoxin, confirming that the type of exchange cation can strongly influences the aflatoxin adsorption on smectites (Deng et al., 2012; Barrientos-Velázquez et al., 2016. Particle size and morphology of the smectite influences the amount of AFB_1 adsorbed, as well (Mulder et al., 2008). A linear correlation (R^2 = 0.73) between the < 2 μm fraction clay content and maximum AFB_1 adsorption was observed. The morphological analysis indicated that the better adsorbents occurred as thin particles, while the moderate to poor adsorbents were observed as thicker particles (Mulder et al., 2008). Recently, Vekiru et al. (2015) showed that the differences in AFB_1 adsorption capacity of smectites can be related to the structural configuration: the *cis*-vacant smectite samples showed higher AFB_1 binding than the *trans*-vacant sample. Notwithstanding these observations, a significant correlation between mineralogical and physico-chemical properties of smectites and AFB_1 adsorption has not been well established. Thereof, a predictive model of AFB_1 adsorption by bentonites does not exist yet, being complicated by the crystal-chemical variability within the smectite group (Tenorio Arvide et al., 2008). So far, the effect of geological origin of bentonites has not been systematically examined. In this contest, the present study was aimed to assess the role of geological origin of bentonites, mined from different locations around the world, on adsorption and retention of AFB_1. In addition, mineralogical and physico-chemical properties of bentonites were determined and correlated to aflatoxin adsorption capacity, affinity and chemisorption index measured by equilibrium adsorption isotherms and toxin desorption studies.

2. Materials and methods

2.1. Chemicals and AFB_1 analysis

AFB_1 standard (purity > 99%) was supplied by Sigma-Aldrich (Milan, Italy). All chemicals used were of analytical grade unless otherwise stated. All solvents were purchased from J.T. Baker (Deventer, The Netherlands) and were of High Performance Liquid Chromatography (HPLC) grade. Water was of Milli-Q quality (Millipore, Bedford, MA). The binding of AFB_1 to bentonites was studied under two different pH conditions: pH3 (citrate buffer), and pH7 (phosphate buffer). These pH values were chosen to determine the effect of pH on mycotoxin binding within the range found in the gastrointestinal tract. Citrate buffer (0.1 mol/L) was prepared by dissolving 4.27 g of tri-sodium citrate 2-hydrate ($C_6H_5Na_3O_7$ – $2H_2O$, MW 294.1) in approximately 900 mL of distilled water. Then, the solution was adjusted to pH3 with 17.96 g of citric acid ($C_6H_8O_7$ – H_2O, MW 210.13, d 1.5) and filled up to 1000 mL with distilled water. To prepare the phosphate buffer (0.1 mol/L), a 0.1 mol/L solution of sodium di-hydrogen phosphate 2-hydrate (NaH_2PO_4 – $2H_2O$, MW 156.01) was prepared by dissolving 15.601 g of NaH_2PO_4 – $2H_2O$ in 1000 mL of distilled water. A 0.1 mol/L solution of di-sodium hydrogen phosphate 12-hydrate (Na_2HPO_4 – $12H_2O$, MW 358.14) was prepared by dissolving 35.814 g of Na_2HPO_4 – $12H_2O$ in 1000 mL of distilled water. Then, the Na_2HPO_4 solution was adjusted to pH7 by adding the NaH_2PO_4 solution.

Stock solutions of AFB_1 (1 mg/mL) were prepared by dissolving the powder of toxin in acetonitrile. Stock solutions were stored in the dark at 4°C. The actual concentration of these stock solutions was verified by UV-vis spectrophotometric according to the AOAC Official Methods of Analysis (2000). Briefly, a standard solution at 10 μg/mL was prepared by properly diluting the stock solution with acetonitrile, and then measuring the absorbance at wavelength of maximum absorption close to 350 nm. The following equation was applied to calculate mycotoxin concentration: Mycotoxin (μg/mL) = (A x MW x 1000)/ε, where A = absorbance (mean of 6 replicate measurements), MW = molecular weight (312 g/mol), ε = molecular absorptivity (20700). To perform the adsorption experiments, working solutions of AFB_1 were prepared by diluting the stock solution (1 mg/mL) with citrate or phosphate buffers.

AFB_1 was analysed by HPLC with fluorometric detection. The HPLC apparatus consisted of an Agilent 1100 series system (Agilent, Waldbronn, Germany) equipped with a binary pump (G1312A model), autosampler (G1313A model), column thermostat (G1316A model) and

a spectrofluorometric detector (G1321A model). The column used was a Zorbax SB-Aq, Agilent (150 x 4.6 mm, 5.0 μm particle sizes). Column temperature was set at 35°C. Isocratic mobile phase consisting of water/acetonitrile (50/50, v/v) was eluted at 1 mL/min flow rate for 4.5 min followed by a 3 min washing step with 90% acetonitrile. The fluorescence detector was set at 365 nm (λ_{ex}) and 435 nm (λ_{em}). AFB_1 retention time was 3.5 min.

2.2. AFB_1 adsorption and desorption experiments

Preliminary adsorption experiments were performed to determine the efficacy of selected bentonites in adsorbing AFB_1 from citrate and phosphate buffers. Adsorption trials were carried out at constant temperature (37°C), using a very little adsorbent concentration set at 0.001% w/v (corresponding to 0.01 mg/mL) and 90 min of contact time. This concentration was preferred as it allowed the ranking of bentonites yielding detectable reduction values of the toxin from the liquid mediums. Briefly, 2 mg of each bentonite sample were weighed in an amber glass vial and suspended with 10 mL of buffered solution. This suspension was vigorously mixed by vortex for a few seconds. Afterwards, 100 μL of the suspension were added to 1.9 mL of standard working solution containing 1 μg/mL of AFB_1. The latter suspension was vigorously mixed by vortex for few seconds and then shaken in a thermostatically controlled shaker (KS 4000, IKA®-Werke GmbH &Co. KG) at constant temperature and 250 rpm speed. After incubation period, 1 mL of suspension was transferred into an Eppendorf tube and centrifuged for 20 min at 18 000 x *g* and 25°C. Supernatant sample was analyzed for the residual mycotoxin content by HPLC. A blank control was prepared using the mycotoxin working solution in buffer without bentonite. This was subjected to the same test procedure and served as background control during the analysis to investigate the stability of toxin in the buffer solutions or any possible nonspecific adsorption. Chemical precipitation and losses of mycotoxins due to nonspecific adsorption were not detected.

Equilibrium adsorption isotherms were performed at 37°C, pH7 and 90 min of contact time testing standard solutions containing an increasing AFB_1 concentration (1-10 μg/mL) with a fixed amount of bentonite (0.005%, w/v). This adsorbent amount was preferred as it yielded for all samples a range of aflatoxin adsorption values suitable for curve fitting and mathematical modeling. All adsorption experiments were performed in triplicate.

In order to investigate the desorption capacity of AFB_1 from bentonite, 10 mg of adsorbent material was weighed into a 2-mL screw-cap test tube and mixed with 2 mL of mycotoxin working solution (pH7), containing 5 μg/mL of AFB_1. Higher adsorbent (0.5% w/v) and toxin concentrations were used for this study to have detectable amounts of toxin in the desorbing solvent. Samples were incubated at 37°C, for 90 min in a rotary shaker as described above, then they were centrifuged, the supernatants completely removed and analysed for residual mycotoxin content. To assess mycotoxin desorption due to methanol, after complete removal of supernatants, the adsorbent pellets were washed twice with 2 mL of methanol, and shaken for 30 min at 250 rpm. The supernatants of methanol desorption steps were pooled and analysed for mycotoxin content. Desorption study was performed in triplicate. Values of mycotoxin adsorption (at pH7) and desorption were calculated and expressed as percentage. The chemisorption index (C_α) was calculated and expressed as the ratio of the difference between the amount of toxin adsorbed (C_b) and the amount desorbed (C_d) to the initial amount (C_i), $C_\alpha = C_b - C_d / C_i$.

2.3. Bentonites and physico-chemical characterization

Bentonite samples (29) in form of thin powder were collected by Laviosa Chimica Mineraria SpA (Livorno, Italy) from different mining companies and were obtained from a variety of locations, including some within the European Union. In particular, one sample was from France (H3), one from Spain (H5), one from Greece (H11), one from Georgia (H7), one from Morocco (H10), two from Italy (H1 and H6), five from India (H8, H9, H12, H13 and H14), five from Argentina (S4, S8, S11, S12 and S13), five from the USA (S5, S9, S10, S14 and S15), and seven from Turkey (H2, H4, S1, S2, S3, S6 and S7). As reported by the providing companies, most samples were mined by stripping methods from open pits after removing any overburden. Uniform samples were obtained by separating the bentonite from a single pit into several stockpiles, which were subsequently blended to obtain the desired composition. According to the manufacturers, extraction of the clays was followed by crushing, drying, and grinding. Samples did not undergo to further processing procedures. Mineralogical and physico-chemical characterization of bentonites, and AFB_1 adsorption trials were performed using "as received" samples. All materials were labeled with a number code and were divided into two main groups, i.e. hydrothermal ("H", n = 14) and sedimentary ("S", n = 15) bentonites. Geological origin of bentonites was assessed by geochemical and geological surveys performed by geological technicians of the mining companies.

The swell index, a test that evaluates the swelling ability of bentonite under zero normal stress, was measured by adding 2 g of finely ground bentonite oven dried at 105°C to 100 mL of reagent water by 0.1 g increments (ASTM D5890, 2011). After a minimum hydration period of 16 h, the volume of hydrated clay mineral was recorded. The swell index was expressed as mL/2 g ± 0.5 mL.

The grade of bentonite was measured by the methylene blue cation-exchange capacity (MBI/CEC) (C837-09, 2014; Taylor, 1985). The results were expressed as mg of methylene blue zero hydrate per gram of dry bentonite. These values were used to calculate the CEC as the total amount of cations absorbed expressed in centiequivalent per Kg of dry sample.

Moisture content was determined according to the ASTM D2216-10 (2010). For this purpose, 20 g of product were weighed precisely to within 0.05 g into a dish, and then dried in the oven at 105°C until a constant weight. The sample was cooled in the desiccator. The percentage of moisture was calculated as C = (A – B)/A x 100 where: A is the sample with moisture in grams, B represent the dried sample in grams and C is the moisture (water content in percentage). The water content was specified within a precision of 0.1%.

The carbonate content was determined using the titration method according to ASTM D4373-14 (2014). A carbon dioxide (CO_2) development was observed following the addition of hydrochloric acid (HCl) to bentonite. The amount of CO_2, gives a measure of carbonate presence in the bentonite (expressed as calcium carbonate). For this purpose, 2–3 grams of material with 0.01 g precision was weighed and poured in a small flask. Inside there was a small test tube with about 10 mL of HCl (1:1). The flask was closed and the burette was leveled to zero. The flask was inclined so that the HCl was in contact with the bentonite and the CO_2, which has developed in the burette, was collected. When stabilized, the flask near the burette was moved until the level of the water was the same than the burette. Then the volume of the CO_2 developed was read.

The loss on ignition (LOI) at 960°C was measured gravimetrically from dry samples (110°C), according to LOI = $(W_d - W_f)/W_d$ x 100, where W_d is the weight of the dry sample at 110°C, and W_f is the weight of the calcined sample at 960°C during 3 h. pH of bentonite samples was measured according to a standard test method (ASTM D4972-18, 2018)

Bentonite samples were characterized by X-ray Fluorescence (XRF) analysis to determinate the amount of the various metals in the original samples (Alshameria et al., 2018; Díaza et al., 2018). 1-2 mL of polyvinyl alcohol (10%) were added to 6-8 g of powder sample and this mixture was put in an oven at 100°C for a couple of hours until dryness. The sample was crushed in a mortar until obtaining a powder without lumps. The sample was put into a sample holder previously partially filled with boric acid, and then pressed through a manual press to obtain a tablet. The amount of metals was determined by an S4 Explorer

X-ray spectrophotometer (Bruker AXS GmbH, Germany) operating at a power of 20 kV and 5 mA. The quantitative results were calculated as oxides and normalized to 100%.

X-ray diffraction (XRD) analysis was performed to determinate the crystalline mineral content in bentonite samples based on the method by Moore and Reynolds (1989). X-Ray diffraction analysis is based on the typical characteristic of crystals to satisfy Bragg's law: $n\lambda = 2d\text{sen}\Theta$ with n being an integer, λ the wavelength of the Cu Kα-radiation, d the repeated distances of the crystal planes (of the smectite) and Θ the angle between the incident x-ray beam and the scattering planes. Diffraction is possible only in the presence of a crystalline system, so this analysis allows the identification of all minerals present in a sample if not in an amorphous state. XRD analysis was performed using the diffractometer Philips type PW1840 (Rigaku, Germany) with the following operating conditions: Cu-Kα radiation, 40 kV voltage, 20 mA current and slit size of 0.2°. The samples were scanned between 2 and 65° 2θ. The step size was 0.02° 2θ and counting time was 1 s/step. Bentonite samples had a residue on 200 mesh (0.075 mm) not exceeding 10%. Moisture of sample powder ranged from 8–12%. The XRD data were analyzed using Jade 7.1.2 software (Jade Software Corp., Christchurch, New Zealand). The data were processed with Excel 2010 (Microsoft Corp., Redmond, WA, USA) and Origin 6.0 software (OriginLab, Northampton, MA, USA). If smectite was present without other minerals the result indicated 100% smectite. If other minerals were present, they were identified. The difference between the percentage of identified minerals and 100% was considered smectite.

Bulk samples were analyzed for particle size by a laser diffraction particle size analyzer (Sympatec, RODOS/IM-VIBRI-HELOS/BF, Sympatec GmbH-System, Germany). This instrument uses laser diffraction technology and multi-wavelength light scattering to determine particle size distribution in a single analysis by virtue of binocular optics. The analysis of optical parameters was performed using the Sympatec software WINDOX 5. Particle size distribution curves were provided by the software.

The viscosity of bentonite dispersions was measured using a Brookfield DV-II prime digital viscometer (Brookfield Engineering Laboratories, INC., MA, USA). Dispersions were prepared with 4% bentonite (w/v) in distilled water and by mechanical mixing for 20 min at 20 000 rpm using a Hamilton Beach mixer. The viscometric data were obtained using a rotational speed at 20 rpm. All rheological tests were performed at 25°C ± 0.1. After mixing, each bentonite dispersion was poured in a covered container and left for a specific time at room temperature. The flow curves of samples were measured at different aging times, namely, immediately after the preparation, and 24h after preparation. In this study, viscosity values measured at time 0 are reported.

2.4. Data calculations of mycotoxin adsorption and statistical analysis

The adsorption is generally defined as the percentage of mycotoxin adsorbed on adsorbent materials related to the quantity present at the beginning of the test, under the test conditions. The amount of adsorbed mycotoxin was calculated as the difference between the amount of AFB_1 in the supernatant of the blank tubes with no test product and the amount found in the supernatant of the experimental tubes with the bentonite. This amount was related then to the quantity present in the supernatant of the blank tubes and expressed as percentage.

Adsorption isotherms were obtained by plotting the amount of AFB_1 adsorbed per unit of mass of adsorbent (Q_{eq}) against the concentration of AFB_1 in the external phase (C_{eq}), under equilibrium conditions (Q_{eq}) = $f(C_{eq})$. These data were transferred to SigmaPlot (Systat.com, version 12.3) and fitted by the Langmuir, the Freundlich and the Sips models (Foo and Hamed, 2010) using the non-linear regression method and the Marquardt-Levenberg algorithm to find the best adsorption parameters, i.e. the maximum adsorption capacity B_{max} (mg/g) and affinity K_d (L/mg) related to the adsorption of AFB_1 onto bentonites. The SigmaPlot nonlinear regression method, which uses the Marquardt – Levenberg algorithm, was used as a viable tool to define the best-fitting relationship between a set of experimental data and the proposed isotherm models. Statistical analysis was performed using a factorial ANOVA with concentration (C_{eq}) as categorical predictor variable and quantity of mycotoxin adsorbed (Q_{eq}) as dependent variable. The normality test (Shapiro-Wilk), the constant variance test (Spearman rank correlation), and the Durbin – Watson statistic test were used to test, respectively, for normally distributed population, constant variance assumption, and correlation between residuals. The threshold for significance level for normality and constant variance test was set at $p < 0.05$. The expected value of the Durbin – Watson statistic for random, independent, normally distributed residuals was 2. The coefficient of determination (R^2), the standard errors of the estimate ($s_{y|x}$), the residual sum of squares (SS_{res}), and the predicted residual error sum of squares (PRESS) were calculated to assess the fitness/suitability of the regression models. The isotherm models that provided the lowest SS_{res}, $s_{y|x}$, and PRESS and the highest R^2 were considered to give the closest fit.

Experimental results relevant to AFB_1 adsorption, AFB_1 desorption and physico-chemical properties of smectites belonging to different geological categories were compared using the t-test analysis. In addition, the Normality test (Shapiro-Wilk) and the Equal Variance test were used to check, respectively, normally distributed population and constant variance assumption. The threshold for significance level for Normality and Equal Variance tests was set at $p < 0.05$. Mann-Whitney Rank Sum Test was used when Normality and/or Equal Variance tests failed.

3. Results and discussion

3.1. Mineralogical composition of bentonites and physico-chemical properties

Bentonite is a widely distributed material and is mined worldwide. However, the main deposits are located in few countries (22) with the USA, Greece, and the Commonwealth of Independent States accounting for roughly 55% of the annual world production (WHO, 2005). For this study, samples were obtained from deposits located in some of the most important bentonite producing areas in the USA, India, Argentina, Turkey, Spain, Italy and Greece. Geological surveys performed *in situ*, and mineralogical and chemical examination of bentonite samples allowed geological technicians of providing companies to divide the deposits into two main groups: *i*) those resulting from sub-aqueous alteration of fine-grained volcanic ash (sedimentary bentonites), and *ii*) those resulting from in situ hydrothermal alteration of volcanic rocks (hydrothermal bentonites) (Grim and Güven, 1978). Samples of sedimentary (15) and hydrothermal (14) bentonites were in equal number, and were all examined for mineralogical and physico-chemical properties, namely mineral, and metal contents, carbonate content, pH, total moisture content, particle size distribution, cation exchange capacity (MBI/CEC), swell index, loss of ignition at 960°C, and viscosity.

XRD analysis provides definitive information on the mineralogical composition of a bentonite, both in terms of clay and non-clay constituents. In addition the d060-value shows whether the smectite is dihoctaedral (1.49-1.50 Å) or trioctahedral (1.52-1.53 Å). Results of mineralogical analysis of bentonite samples are summarized in Table 1A (sedimentary bentonites) and 1B (hydrothermal bentonites). The major mineral identified in each of the twenty-nine natural samples was found to belong to the smectite group with dioctahedral structure (montmorillonite), as suggested by the XRD peak at 1.493-1.500 Å (d060-value). Other minerals were found in subordinate quantities (Table 1A and B). The major accessory mineral in the samples was quartz. Feldspars, calcite, opal/cristobalite, mica, kaolinite, gypsum, zeolite, hematite, heulandite or dolomite were also found. Carbonate content was low being less than 6.5%, except for the hydrothermal bentonite H3 sample which contained 12.6% of carbonate. XRD

Table 1
Mineralogical and chemical properties of sedimentary (A) and hydrothermal (B) bentonites.

A: Sedimentary bentonites

	S1	S2	S3	S4	S5	S6	S7	S8	S9	S10	S11	S12	S13	S14	S15
Type of smectite*	Na	Na	Na	Semi-Na	Ca	Na	Na	Na	Na	Na	Na	Na	Semi-Na	Na	Na
Subordinate minerals	Quartz Feldspars Calcite Opal Cristob. Zeolite	Feldspars Calcite Opal Cristob. Quartz Heulandite Biotite	Quartz Calcite Opal Cristob. Feldspars Heulandite Biotite	Quartz Feldspars Calcite Opal Cristob.	Quartz FeldsparsCalcite Mica	Quartz Feldspars Calcite Opal Cristob. Mica	Feldspars Opal Cristob. Mica Calcite Quartz Zeolite	Feldspars Calcite	Quartz Feldspars Mica	Quartz Feldspars Opal Cristob. Gypsum	Quartz Feldspars Gypsum Calcite	Quartz Opal Cristob.	Quartz Feldspars	Quartz Feldspars Opal Cristob. Gypsum	Quartz Cristob. Gypsum
d001	12.600	12.460	12.583	13.010	14.672	12.654	12.370	12.690	11.760	11.530	12.369	12.510	12.860	12.690	12.201
d060	1.497	1.496	1.499	1.496	1.497	1.498	1.497	1.499	1.497	1.493	1.497	1.498	1.499	1.497	1.498
Na_2O (%)	1.94	2.01	2.23	1.42	0.22	1.8	1.7	2.56	1.76	1.65	2.63	1.91	1.49	1.69	1.64
MgO (%)	2.07	2.18	2.14	2.26	3.71	2.24	2.07	3.21	1.58	2.37	2.87	3.35	2.13	2.38	2.51
Al_2O_3 (%)	17.85	18.93	17.43	17.62	18.32	18.29	17.95	19.71	18.49	19.96	19.45	20.15	17.32	19.26	19.4
SiO_2 (%)	61.81	58.51	60.75	59.4	56.33	61.67	62.71	61.35	65.70	61.27	58.79	61.38	60.99	63.55	62.88
P_2O_5 (%)	0.13	0.19	0.11	0.13	0.07	0.1	0.13	0.06	0.04	0.05	0.09	0.05	0.28	0.05	0.04
K_2O (%)	1.91	1.88	1.92	2.21	1.82	1.81	1.77	1.54	1.79	1.76	1.64	1.50	2.21	1.73	1.59
CaO (%)	2.75	4.12	2.67	3.23	4.65	2.98	2.76	0.23	1.08	1.38	1.46	0.27	1.31	1.25	1.2
TiO_2 (%)	0.32	0.35	0.33	0.57	0.84	0.37	0.34	0.44	0.15	0.21	0.76	0.44	0.67	0.16	0.17
MnO (%)	0.13	0.17	0.12	0.09	0.06	0.09	0.12	0.02	0.01	0.05	0.07	0.03	0.09	0.04	0.01
Fe_2O_3 (%)	3.94	4.27	3.91	5.68	5.47	4.32	4.11	4.66	4.57	5.23	5.8	4.57	7.51	4.32	4.05
Carbonate (%)	4.86	6.4	4.78	3.29	3.24	4.62	3.83	0	0.63	1.28	0.31	0	0.66	0.98	0.61

B: Hydrothermal bentonites

	H1	H2	H3	H4	H5	H6	H7	H8	H9	H10	H11	H12	H13	H14
Type of smectite*	Ca	Ca	Semi-Na	Ca	Ca	Ca	Ca	Semi-Na	Semi-Na	Ca	Ca	Semi-Na	Semi-Na	Semi-Na
Subordinate mineral	Feldspars Mica Quartz	Opal Cristob.	Quartz Calcite Kaolinite Gypsum Feldspars	Quartz Kaolinite Zeolite	Quartz Kaolinite Mica Dolomite Feldspars Calcite	Quartz Feldspars Calcite Hematite	Mica Quartz Feldspars Opal Calcite	Calcite Quartz Hematite	Quartz Calcite Gypsum Hematite Feldspars	Feldspars Mica Quartz	Quartz Opal Cristob. Feldspars	Calcite Quartz Feldspars Zeolite Hematite	Quartz Feldspars Calcite Hematite	Quartz Feldspars Calcite Opal Cristob. Hematite
d001	14.967	15.540	14.923	16.114	14.520	14.768	15.696	12.729	14.383	14.623	14.917	13.762	13.150	12.710
d060	1.500	1.499	1.493	1.499	1.498	1.499	1.499	1.499	1.500	1.493	1.496	1.500	1.496	1.500
Na_2O (%)	0.7	0.42	1.05	0.27	0.32	0.68	0.3	2.57	0.89	1.74	0.55	1.37	1.12	1.39
MgO (%)	5.51	3.87	2.71	3.81	3.55	4.76	3.59	2.78	2.71	2.45	2.28	3.58	2.74	2.43
Al_2O_3 (%)	17.03	16.02	17.25	19.36	18.53	17.49	18.74	17.13	14.83	23.31	14.11	17.62	15.04	14.79
SiO_2 (%)	58.89	69.34	57.06	56.07	54.7	56.7	58.88	49.03	50.87	58.53	72.07	53.14	51.45	54.4
P_2O_5 (%)	0.11	0.02	0.16	0.09	0.11	0.19	0.11	0.25	0.4	0.05	0.03	0.12	0.29	0.26
K_2O (%)	2.12	0.53	2.84	2.26	2.68	2.47	1.57	1.45	1.49	2.23	1.89	1.57	1.46	1.53
CaO (%)	1.77	1.83	9.07	2.56	4.66	2	3.77	2.14	2.97	1.39	1.06	2.5	3.03	1.56
TiO_2 (%)	0.6	0.13	0.53	0.49	0.5	0.73	0.38	1.22	1.68	0.24	0.26	0.93	1.37	1.51
MnO (%)	0.23	0.13	0.15	0.06	0.11	0.11	0.18	0.08	0.1	0.01	0.02	0.08	0.28	0.04
Fe_2O_3 (%)	5.74	1.59	4.16	5.82	5.99	7.15	3.76	13.44	16.22	3.41	2.12	11.13	15.25	15.22
Carbonate (%)	0	0.02	12.55	2.44	6.99	1.4	2.3	3.51	2.01	0.31	0.73	2.19	2.92	1.04

* All samples contained smectite as dominant mineral

examination of an "oriented" mount of the smectite constituent shows whether this contains mainly divalent or monovalent exchangeable cations. Under normal relative umidity, the 001 reflection (d001-value) of a divalent cation saturated-smectite is about 15.4 Å, whereas for a monovalent cation-saturated smectite is about 12.6 Å. Sedimentary bentonites (except samples S4, S5, and S13) showed d001-values ≤12.6 Å, and they were identified as sodium smectites (Table 1A). Sample S5 was a calcium smectite as indicated by its d001-value at 14.7 Å, while samples S4 and S13 were smectites with a mixed sodium/calcium assemblage (sodic-calcic smectites). In the group of hydrothermal bentonites, eight natural samples were calcium dominated smectites, while samples H3, H8, H9, H12, H13 and H14 were identified as sodic-calcic mixed smectites (Table 1B).

XRF is nowadays a frequently used method in analysis of solid geological and environmental materials. The method is fast and cost-effective, because the sample decomposition is not required. XRF results are summarized in Table 1A-B. The main chemical elements which characterized the various bentonite samples were silicon (SiO_2), aluminium (Al_2O_3) and iron (Fe_2O_3), which were calculated on the oxide compound. Sodium (Na_2O), calcium (CaO), potassium (K_2O), magnesium (MgO), phosphorus (P_2O_5), titanium (TiO_2) and manganese (MnO) were found in small quantities (less than 5.5%). It is proposed that only elements of sodium, calcium and potassium are exchangeable. Ranges (and median values in brackets) for some elements in the group of sedimentary bentonites were 7-85 (57) meq/100g for sodium; 8-166 (52) meq/100g for calcium; 33-184 (111) meq/100g for magnesium, and 127-282 (162) meq/100g for iron. In the group of sedimentary bentonites, a low amount of sodium (7 meq/100g) and a high amount of calcium (166 meq/100g) was observed for the sample S5 (which was identified as a calcium smectite). Ranges (and median values) for these elements in hydrothermal bentonites were 9-83 (26) meq/100g for sodium; 38-323 (83) meq/100g for calcium; 113-274 (157) meq/100g for magnesium, and 60-609 (221) meq/100g for iron. As shown in the box blot in Fig. 1, a significant difference in elemental composition between sedimentary and hydrothermal bentonites was found for the contents in sodium and magnesium. As expected, sodium content in sedimentary bentonites was significantly higher than hydrothermal samples (*pt-test* = 0.001), whereas magnesium content was significantly higher in hydrothermal samples (*pt-test* = 0.002). The mean contents of calcium and iron of hydrothermal samples were higher than sedimentary bentonites, but these differences were not significant (*pt-test* = 0.05). Interestingly, most sodic-calcic mixed smectites (namely samples H8, H9, H12, H13 and H14) belonging to the group of hydrothermal bentonites showed the highest content of iron (418-609 meq/100g).

In accordance with chemical element analysis, sedimentary bentonites (being mainly sodium smectites) showed the highest swelling properties, and when mixed with water they exhibited the greatest grade of dispersion. For sedimentary and hydrothermal bentonites, swell index values were in the ranges 9-50 and 3-24 mL/2g, respectively (Tables 2A-B and Fig. 1). Median values of swell index (25^{th} and 75^{th} percentile) were 23 (21-31) mL/2g for sedimentary bentonites, and 9 (5-18) mL/2g for hydrothermal bentonites. These values were statistically different (*pt-test* < 0.001). The calcium-dominant smectite (S5) in the group of sedimentary bentonites exhibited low swelling property, while the opposite was found for the sodic-calcic mixed smectites belonging to the hydrothermal group (namely samples H8, H9, H12, H13 and H14).

Sedimentary and hydrothermal bentonites did not differ substantially in the values of pH (Tables 2A-2B). For all natural samples the pH was in the range of 6.8-9.6, although most of them showed a pH near neutral. It is not uncommon to find alkaline pH values with various aluminosilicates, as well as in confirmed smectite-containing products (Marroquın-Cardona et al., 2009). The US Pharmacopeia has reported a pH of 9.5–10.5 for natural bentonites and 9.0–10.0 for some pure bentonites (montmorillonites) (US Pharmacopoeia, 2005). In general, according to Dixon et al. (2008), "good" AFB_1 adsorbing bentonites should have moderate dispersion and acidity, since extremely high pH promotes particle dispersion and disorder, and extreme acidity promotes excessive aluminum mobilization.

Total moisture content of bentonites was in the range 6-13% (Tables 2A-B), and the differences may be related to batch to batch variations of the samples. In addition, for each natural sample of bentonite, loss of ignification at 960°C was lower than 10% suggesting a low/moderate organic matter content (Tables 2A-B). The organic matter content influences smectite quantitative estimates and may reduce aflatoxin adsorption. Organic substances into the bentonite samples are weak aflatoxin binders and reduce the smectite content in the samples thus negatively affecting their adsorbing efficiency (Dixon et al., 2008).

Although a correlation between aflatoxin adsorption efficacy of bentonites and CEC has not been found (Vekiru et al., 2007), it has been stated that CEC values, and then smectite content of bentonites affect the extent of toxin adsorption (Dixon et al., 2008). Several studies confirmed that an effective aflatoxin adsorbing bentonite should have a CEC value at 70 cmol/kg (Dixon et al., 2008). Most bentonite samples screened in our study showed a CEC value ≥70 cmol/kg (Tables 2A-B). In particular, for the two groups of hydrothermal and sedimentary bentonites, CEC values were in the ranges of 60-116 and 74-102 cmol/kg, with median values (25^{th} and 75^{th} percentile) at 94 (90-97) and 104 (85-111) cmol/kg, respectively. These values did not differ (*pt-test* > 0.05) (Fig. 1) and were within the range reported for bentonite samples acting as good aflatoxin adsorbents (Kannewischer et al., 2006; Vekiru et al., 2007, 2015; Marroquin-Cardona et al., 2009).The CEC is a direct indication of bentonite grade and it measures the accessible anionic sites of the mineral clay. High CEC values reflect the high capacity of the clays to potentially exchange/interact with diverse cationic components. In our study, the CEC was determined using the methylene blue CEC method as described in the methodology. For a number of reasons mainly connected with the large size of the methylene blue ion, this test does not measure the "true" CEC of a bentonite (Taylor, 1985). It is demonstrated that methylene blue index (MBI) commonly underestimates the CEC of untreated expandable smectites by 80%. However, the test is sensitive to the smectite content and has the advantage of being relatively rapid.

In order to avoid the effect of particle size on AFB_1 adsorption, all natural samples were finely ground and sieved to obtain samples with uniform particle size (< 45μm) as described by Grant and Phillips (1998). As shown in Tables 2A-B, all batch samples showed uniform and fine particle size, being the parameter X_{50} (median value of the particles distribution) lower than 40 μm. Median values of X_{50} calculated for the samples belonging to the groups of sedimentary and hydrothermal bentonites were 13 and 19 μm, respectively; and they were not significantly different (*pt-test* > 0.05). Thereof, in our study it is supposed that differences in aflatoxin adsorption of bentonites may not be due the particle size of samples.

Clay is a mineral, either rock or soil, that becomes "plastic" when wet. This property is the results of the small particle size and the plate like nature of the particles. The viscosity values of bentonites measured at 4% bentonite (w/v) in distilled water, 20 000 rpm and time 0 are listed in Tables 2A-B. Median values of viscosity determined for the groups of sedimentary and hydrothermal bentonites were 0.0043 and 0.003 Pa s, respectively. Each group of bentonites included an outlier, that is a sample with a very high viscosity value, namely the samples H8 (0.140 Pa s) and S8 (0.187 Pa s). These samples bear the highest swelling value determined for each group of bentonites (24 and 50 mL/2g, respectively).

In conclusion, overall results suggest that the two main categories of bentonites analysed herein differed significantly in some physico-chemical properties. It was hypothesized that these properties may play a role in differing bentonites to adsorb AFB_1.

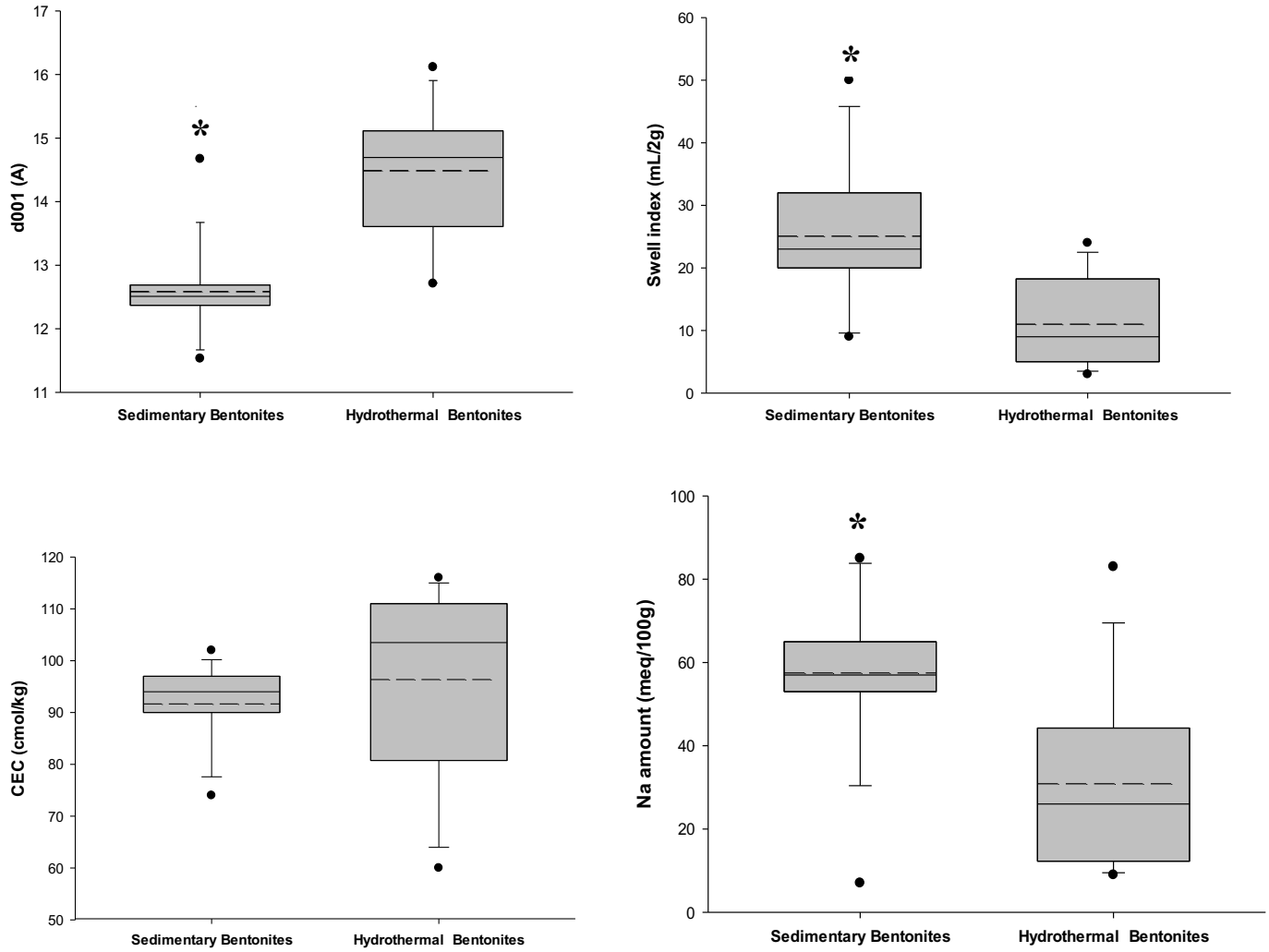

Fig. 1. Distribution of d001-values, swell index, CEC, Na content, Mg content, Fe content and X_{50} values measured for sedimentary and hydrothermal bentonites. The mean and median values are marked by dotted and black lines, respectively. The superscript * in each box plot indicates statistical difference between the two groups of bentonites ($p_{t\text{-}test} < 0.001$).

3.2. Single-concentration and isothermal AFB_1 adsorption experiments

Preliminary experiments of AFB_1 adsorption were performed using a very low adsorbent concentration (0.001% w/v) to differentiate between samples and to identify adsorbing agents with high adsorption capacity. These experiments were performed at pH3 and pH7 to simulate physiological pH values of stomach and intestine in monogastric animals. Extreme acid pH values (pH < 3) were avoided to prevent the conversion of AFB_1 to AFB_{2a}. As remarked by Vekiru et al. (2007), when *in vitro* tests are performed at strongly acidic conditions (pH < 2), AFB_1 can be converted into AFB_{2a}, which might result in misleading assumptions of high adsorption levels. Such a conversion was not observed in our study. AFB_1 adsorption values expressed as percentage and recorded for the two groups of bentonites with different geological origin are listed in Fig. 2. For hydrothermal bentonites, AFB_1 adsorption values recorded at pH3 and pH7 were in the ranges of 0-72 and 2-42%, with median values (25^{th} and 75^{th} percentile) at 27% (9-43%) and 27% (6-31%). AFB_1 adsorption values measured for sedimentary bentonites at pH3 and pH7 ranged as 25-92 and 18-79%, with median values (25^{th} and 75^{th} percentile) at 77 (52-87%) and 52 (42-60%). Within the two groups of bentonites and for most samples, AFB_1 adsorption recorded at acid pH was higher than adsorption obtained at neutral pH. Interestingly, although the two groups of bentonites contained smectite as major mineral constituent they differed substantially in their AFB_1 adsorption behavior. As shown in the box plot of Fig. 3, the removal of AFB_1 from buffered mediums was highly dependent on the geological origin, which likely guaranteed some particular physico-chemical properties to the minerals. Both at pH3 and at pH7 of the medium, sedimentary bentonites adsorbed significantly higher amounts of AFB_1 than hydrothermal bentonites ($p_{t\text{-}test} < 0.001$).

To better discriminate between smectite samples for AFB_1 adsorption efficacy, all samples were analyzed by equilibrium adsorption isotherms. Adsorption isotherm experiments were performed using a low adsorbent concentration (0.005% w/v), and at neutral pH. The use of isotherms is one of the most efficient mathematical approaches to describe surface adsorption, in which the amount of compound adsorbed per unit of mass of adsorbent is plotted against the concentration of the compound in the external phase, under equilibrium conditions. Adsorption isotherm equations are used to study the nature of adsorption. These isotherms are characterized by parameters that express the surface properties and affinity of the adsorbent towards different adsorbates (Foo and Hameed, 2010). The shapes of these model isotherms depend on the type of adsorbate/adsorbent and the intermolecular interactions between the fluid and the surface. The model that fits the experimental data most accurately can then be used to describe the system and predict the adsorption behaviour. In this study, three, out of the several equations published to study the isotherm adsorption of mycotoxins to organic and inorganic adsorbent materials, provided the

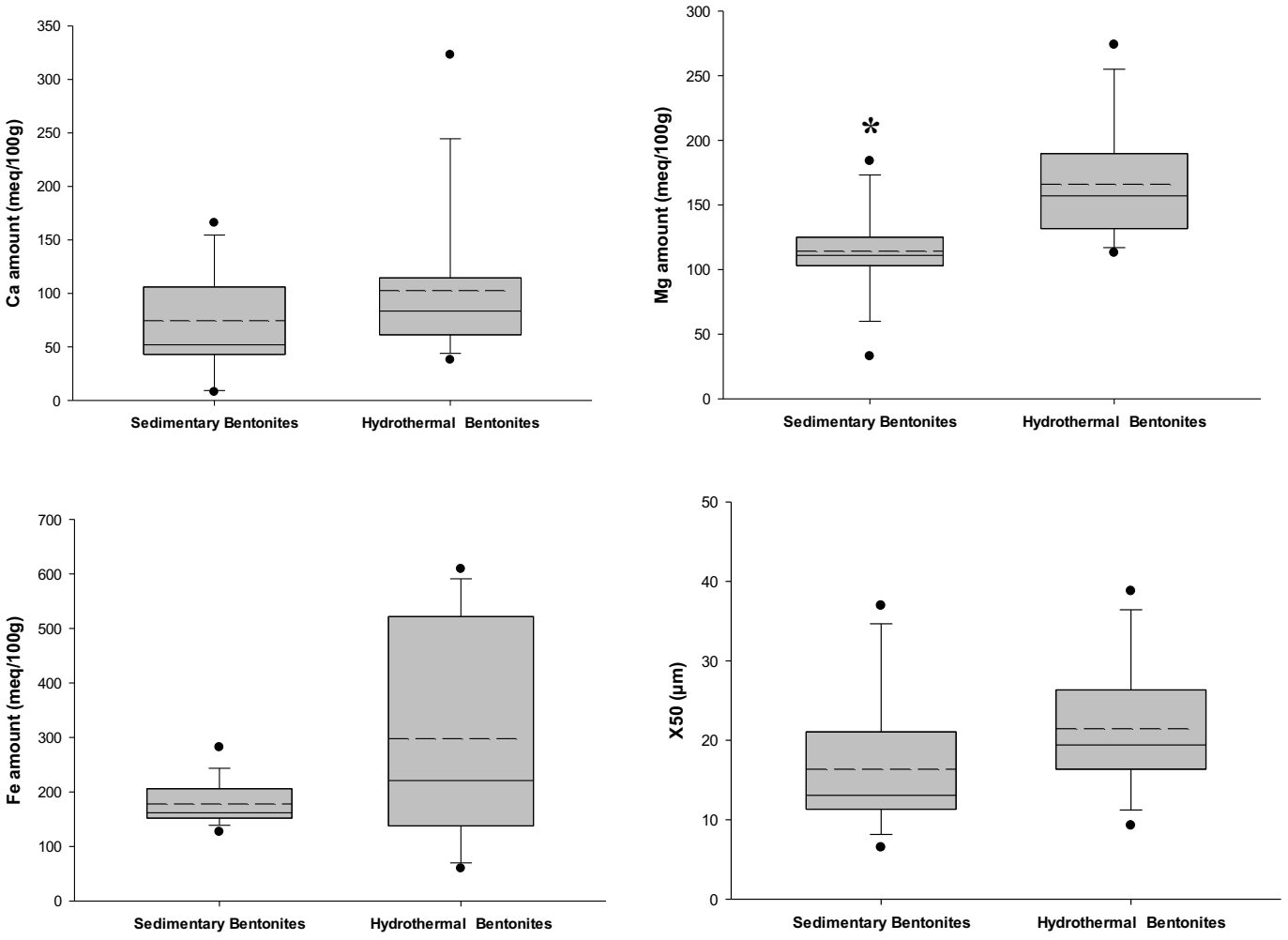

Fig. 1. (*continued*)

best description of AFB_1 adsorption by selected smectites: the Freundlich, the Langmuir, and the Sips models (Foo and Hameed, 2010). Taking into account the number of samples (29), 29 adsorption plots and 87 nonlinear correlations (three isotherm models for each adsorption plot) were performed. The experimental and predicted isotherms for AFB_1 adsorption by bentonites belonging to the two different geological groups are shown graphically in Fig. 4. In most isotherm plots, the amount of AFB_1 adsorbed per unit mass of bentonite increased gradually by increasing AFB_1 molecules in the working solution. Isotherms showed an exponential relationship and a typical L-2 or L-1 (Langmuir) shape. Predicted adsorption isotherms were obtained by fitting experimental adsorption data with the best equation. The nonlinear regression analysis method, instead of the linear regression with transformed variables, was preferred to assess the goodness of the fits and to calculate the parameters involved in the adsorption mechanism (Motulsky and Ransnas, 1987). Transformations of nonlinear isotherm equations to linear forms implicitly alter their error structure and may also violate the error variance and normality assumptions of standard least squares. As in previous studies (Avantaggiato et al., 2014; Greco et al., 2018), the best fitting isotherm equation was found by the measurement of standard error statistics (namely, SS_{res}, $s_{y|x}$, and predicted residual sum of squares PRESS) and of the nonlinear correlation coefficient R^2. The smaller the SS_{res}, $s_{y|x}$, and PRESS, the closer the isotherm models (and the related curves) matched the experimental adsorption data. Among the tested isotherm equations, the better representation for the experimental results of the AFB_1 adsorption isotherms was obtained using the Langmuir and the Sips models ($R^2 > 0.920$ with low error values). These models allowed the calculation of the adsorption parameters, B_{max} and K_d, which allowed us to rank bentonites on their efficacy in adsorbing AFB_1. Interestingly, both adsorption parameters (B_{max} and K_d) showed a meaningful relationship to the AFB_1 adsorption and were considered for the study. In accordance with the results of preliminary adsorption experiments, the comparison of AFB_1 adsorption parameters calculated for hydrothermal and sedimentary bentonites (Table 3) showed that sedimentary bentonites were superior in the binding of the toxin. Theoretical values of B_{max} and K_d calculated for sedimentary bentonites were significantly higher than those determined for hydrothermal bentonites ($p_{t\text{-}test} < 0.001$) (Fig. 5). B_{max} values of sedimentary and hydrothermal bentonites were in the ranges 78.8-164.5 and 36.5-126.1 µg/mg, respectively (Table 3, Fig. 5). The values of median (25^{th} and 75^{th} percentile) were 124.7 (105.7-135.9) µg/mg for sedimentary bentonites; and 77.4 (54.7-99.9) µg/mg for hydrothermal bentonites. In accordance with previous studies (Dixon et al., 2008), our results show that good performing bentonites for AFB_1 reduction (sedimentary bentonites) have a B_{max} value higher than 100 µg/mg (0.32 mol/kg), while worst bentonites (hydrothermal bentonites) show a B_{max} value lower than this threshold. The trend of the Langmuir parameter K_d was in line with B_{max}, being > 1 L/mg (312 500 L/mol) for sedimentary bentonites, and < 1 L/mg for hydrothermal bentonites (Table 3, Fig. 5). In particular, the K_d of sedimentary and hydrothermal bentonites was in the ranges 0.2-5.6 and 0.0-3.3 L/mg, respectively (Table 3). The values of median (25^{th} and 75^{th} percentile) were 1.9 (1.6-3.2) L/mg for sedimentary bentonites; and 0.6 (0.3-1.0) L/mg for hydrothermal bentonites (Table 3,

Table 2
Physical properties of sedimentary (A) and hydrothermal (B) bentonites

A: Sedimentary bentonites

	S1	S2	S3	S4	S5	S6	S7	S8	S9	S10	S11	S12	S13	S14	S15
pH	9.4	9.1	9.4	8.2	7.3	9.4	9.0	7.8	8.3	8.3	-	6.0	7.4	8.4	9.5
Moisture (%)	5.9	7.6	5.6	5.8	9.6	9.9	6.3	10.0	4.4	5.7	8.6	10.4	5.8	9.4	6.6
Dry residue > 45 μm (%)	5.2	0	0.1	0.5	39.2	0.05	2.8	24.7	1.0	1.9	40.8	23.8	2.3	0	0
X_{50} (μm)	14.14	8.49	40.17	12.03	32.37	11.54	14.86	21.06	11.13	12.66	36.95	-	13.50	9.78	6.52
Swell index (mL/2g)	23	23	20	10	9	22	24	50	22	32	25	43	15	26	32
MBI/CEC (cmol/kg)	85	90	80	98	94	90	94	102	74	99	96	97	95	90	91
LOI (%)	7.16	7.40	8.4	7.39	8.51	6.32	6.34	6.22	4.67	6.08	6.43	6.36	5.99	5.57	6.51
Viscosity * (Pa s)	9.3	2.4	4.8	1.8	2	4.2	10.2	187.2	2.4	6.6	-	1.5	7.2	4.5	3.6

B: Hydrothermal bentonites

	H1	H2	H3	H4	H5	H6	H7	H8	H9	H10	H11	H12	H13	H14
pH	6.8	7.2	7.7	7.5	7.3	7.8	7.6	9.6	8.0	7.8	7.7	8.5	8.7	8.3
Moisture (%)	10.2	11.1	5.9	8.6	7.3	10.2	13.4	10.3	9.6	8.4	6.8	9.3	7.0	6.9
Dry residue > 45μm (%)	7.6	0.8	35.0	34.4	35.5	9.5	-	40.7	6.4	12.0	0.1	6.4	3.5	1.4
X_{50} (μm)	18.76	13.18	25.13	25.48	28.90	19.96	38.79	34.07	17.28	20.04	9.28	16.83	16.41	13.21
Swell index (mL/2g)	5	8	4	3	9	5	7	24	14	10	9	19	18	21
MBI-CEC (cmol/kg)	111	102	60	85	68	105	106	97	111	101	68	116	105	114
LOI (%)	7.30	6.11	5.04	9.20	8.85	7.71	8.72	9.9	7.84	6.64	5.59	7.91	7.97	6.86
Viscosity * (Pa s)	2.4	-	7	0.9	3	1.8	-	140	16.5	7.8	3.9	1.2	2.7	3

* Values of viscosity have to be multiplied for 10^{-3}

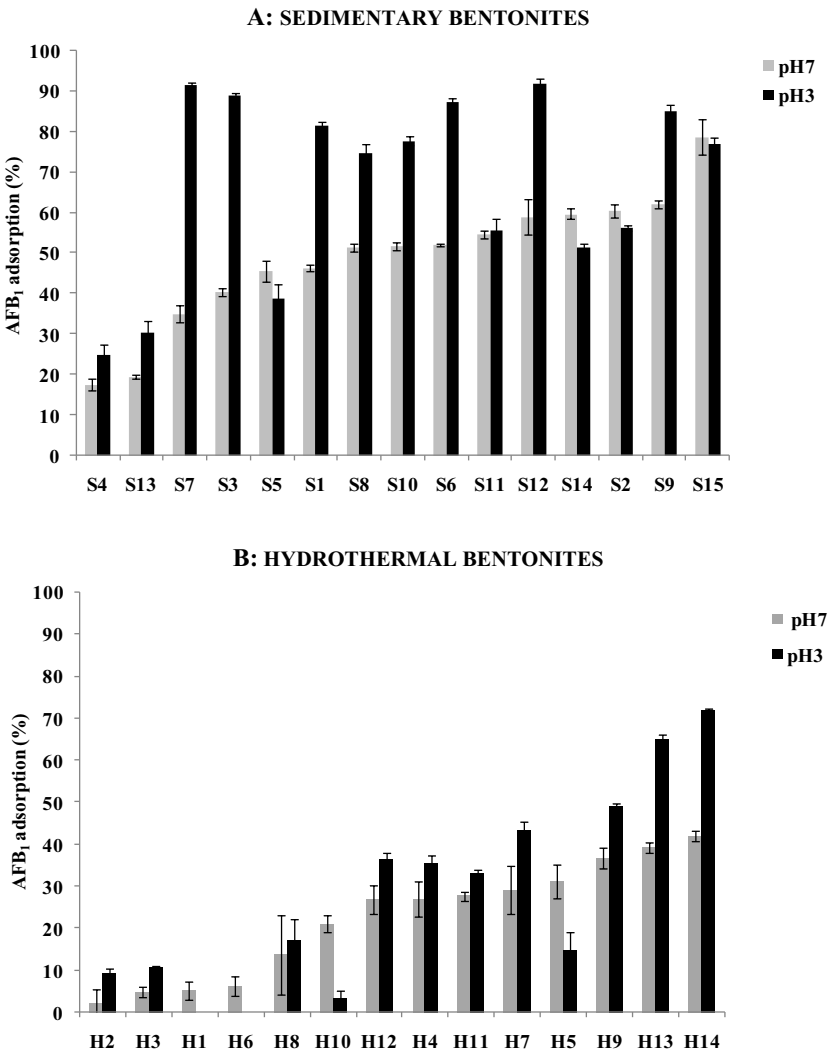

Fig. 2. AFB_1 adsorption values measured for sedimentary (A) and hydrothermal (B) bentonites by preliminary adsorption experiments performed at pH3 and pH7. Bars represent mean values, and error bars are standard deviations of triplicate independent experiments

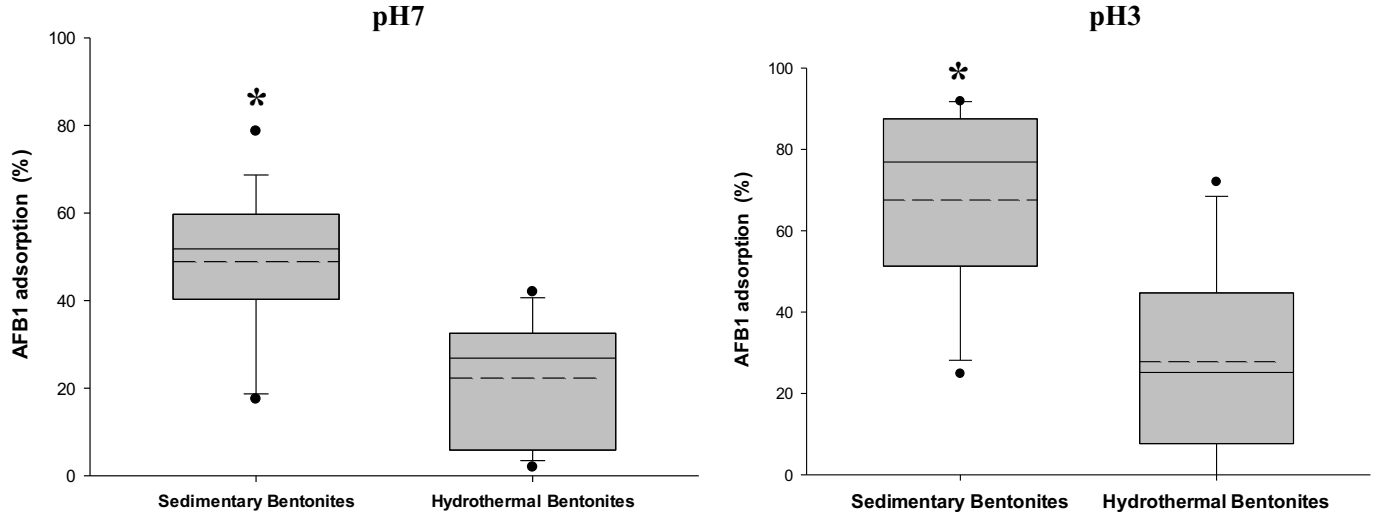

Fig. 3. Distribution of AFB_1 adsorption values measured for sedimentary and hydrothermal bentonites by preliminary adsorption experiments performed at pH7 and pH3. The mean and median values are marked by dotted and black lines, respectively. The superscript * in each box plot indicates statistical difference between the two groups of bentonites ($p_{t\text{-}test} < 0.001$).

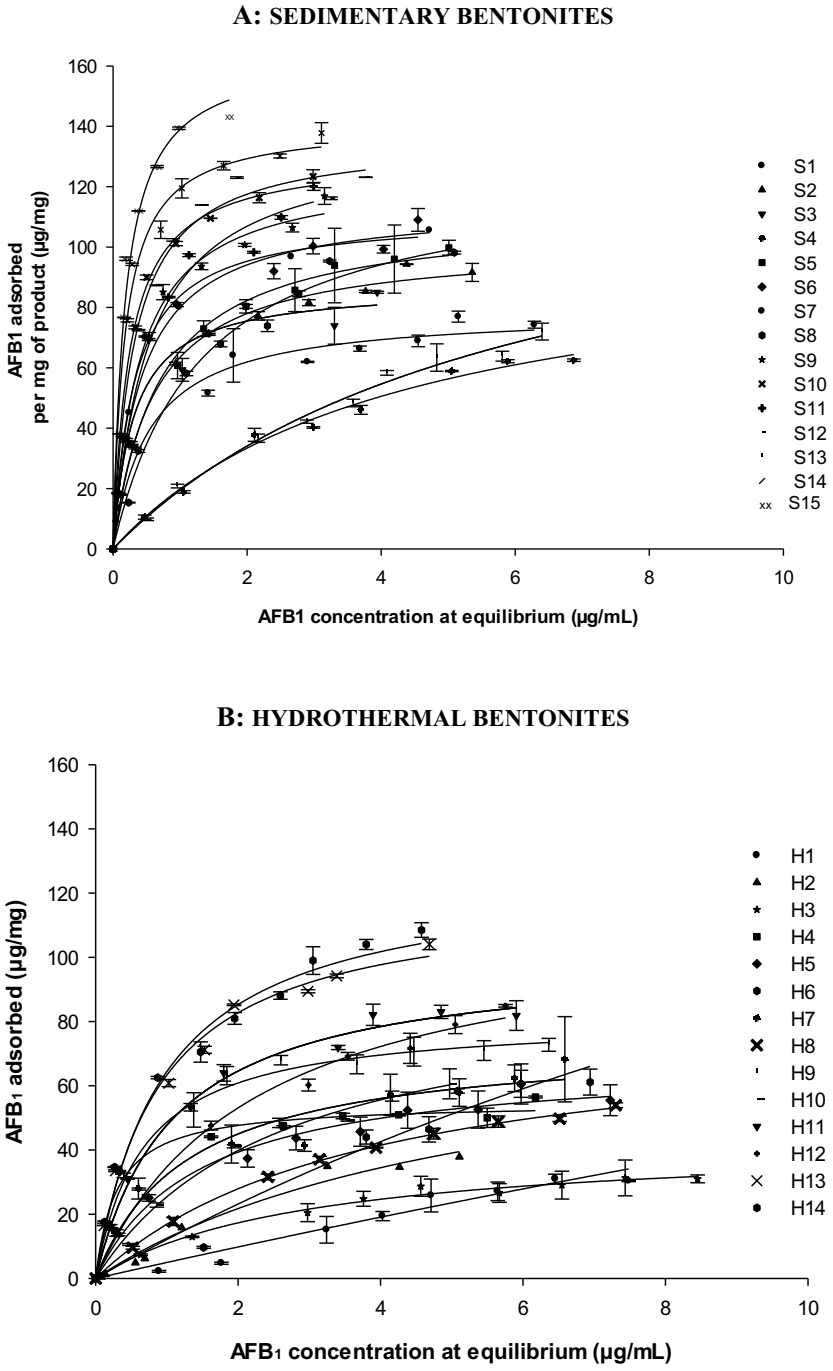

Fig. 4. AFB_1 adsorption isotherms obtained for sedimentary (A) and hydrothermal (B) bentonites. Experimental adsorption data were fitted using the best mathematical model (the Langmuir or the Sips model).

Fig. 5).

Taking into account the strong relationship between the results of preliminary and isothermal adsorption studies, we correlated isothermal adsorption parameters calculated for all samples to relevant adsorption values expressed as percentage (Ads%). The data from these studies were shown to be normally distributed, and both a Pearson's correlation and a linear regression analyses were performed. Significant positive correlation values at the 0.05 level were found for B_{max} with Ads% (correlation coefficient (CC) = 0.788, $p < 0.001$), and for K_d with Ads% (CC = 0.769, $p < 0.001$). As shown in Fig. 6, a linear relationship was found between these experimental values with the following linear equations: B_{max} = 54,964 + (1,297 *Ads%) (R^2 = 0.621, $p < 0.001$), and K_d = -0,484 + (0,0590 * Ads%) (R^2 = 0.592, $p < 0.001$). This is the first time that adsorption data obtained by different approaches are correlated, and it can be helpful for a faster screening of bentonites for AFB_1 adsorption efficacy. That is, a simple adsorption test performed using stringent experimental conditions (very low adsorbent concentration) can provide some information on the features of the adsorption. However, the results of these correlations are not conclusive and a bigger number of samples needs to be analysed.

3.3. AFB_1 desorption studies

In addition to AFB_1 adsorption studies, all samples were tested by a

Table 3
AFB_1 adsorption parameters (B_{max} and K_d) calculated by adsorption isotherms for sedimentary (A) and hydrothermal (B) bentonites. Values are means ± standard deviations of triplicate independent experiments.

A: Sedimentary bentonites

	B_{max} (μg/mg)		K_d (L/mg)	
	Mean	SD	Mean	SD
S1	79	2	1.8	0.3
S2	101	2	1.7	0.1
S3	103	7	1.8	0.5
S4	104	6	0.20	0.01
S5	111	4	1.5	1.1
S6	111	2	3.1	0.2
S7	114	2	2.3	0.1
S8	125	4	0.8	0.1
S9	125	3	2.5	0.2
S10	130	2	4.0	0.2
S11	136	4	1.9	0.2
S12	136	4	3.2	0.4
S13	138	10	0.20	0.01
S14	141	2	5.6	0.4
S15	165	8	5.4	0.8

B: Hydrothermal bentonites

	B_{max} (μg/mg)		K_d (L/mg)	
	Mean	SD	Mean	SD
H1	37	4	0.01	0.01
H2	39	1	0.50	0.01
H3	43	3	0.3	0.1
H4	55	1	3.3	0.5
H5	68	4	0.7	0.1
H6	71	6	0.01	0.01
H7	74	6	0.8	0.2
H8	81	2	0.30	0.01
H9	81	2	1.5	0.1
H10	92	6	0.4	0.1
H11	100	2	0.9	0.1
H12	113	5	0.40	0.01
H13	119	3	1.1	0.1
H14	126	4	1.0	0.1

desorption assay to gather more information on their ability in binding the toxin with strength. Table 4 lists adsorption values recorded at pH7 using a high adsorbent concentration (0.5% w/v), and relevant desorption values by methanol. The values of chemisorption index (C_α) are also reported. A value of $C_\alpha = 1$ indicates total binding with no toxin desorption from the binder, while a $C_\alpha = 0$ indicates total toxin desorption from the binder. Due to the high amount of binder used in the test, adsorption values were almost all > 90% (Table 4). C_α values calculated for sedimentary and hydrothermal bentonites were in the ranges 0.35-0.90 and 0.20-0.86, respectively. Median values (25^{th} and 75^{th} percentile) were 0.66 (0.56-0.83) and 0.46 (0.33-0.61) for sedimentary and hydrothermal bentonites. As observed for AFB_1 adsorption results, the mean values of toxin desorption determined for the two groups of bentonites were significantly different ($p_{t\text{-}test} = 0.021$) (Fig. 7). These findings suggest that sedimentary bentonites adsorb AFB_1 more efficiently than hydrothermal bentonites and keep bound the adsorbed fraction. In accordance with previous studies (Kannewischer et al., 2006; Vekiru et al., 2007), good AFB_1 binders, that is sedimentary bentonites in our case, adsorbed high amounts of toxin from the medium and did not release the toxin when the complex adsorbent:toxin was extracted by methanol. Indeed, a significant linear correlation was found for overall adsorption values obtained by the preliminary single concentration adsorption study (pH7) *versus* C_α [Ads % = 1,801 + (63,171 * C_α); $R^2 = 0.483$, $p < 0.001$) (Fig. 8).

3.4. Correlation between physico-chemical properties of bentonites and AFB_1 adsorption efficacy

Correlation studies were carried out to determine a relationship among the physico-chemical properties and the amounts of toxin that were adsorbed/desorbed by all bentonites. Thereof, the AFB_1 adsorption values recorded at pH3 and pH7 by the preliminary adsorption tests, and the B_{max} values determined at pH7 by the isothermal adsorption studies were correlated with some chemical (CEC, sodium, calcium, magnesium and iron contents) and physical (swell index and basal spacing) properties of bentonites (Table 5). Overall results ($n = 29$) were found normally distributed without outliers and were used for Pearson's correlation statistical analysis. At both pH values considered herein, AFB_1 adsorption values in percentage positively correlated with swell index ($CC = 0.669$ and 0.710 at pH7 and 3) and sodium content ($CC = 0.485$ and 0.481 at pH7 and pH3). In accordance with these results, a positive correlation was found between B_{max} and swell index ($CC = 0.712$), and between B_{max} and sodium content ($CC = 0.551$). These correlations were found very significant, being p values < 0.001 (Table 5). Significant linear regressions ($p < 0.007$) were also obtained comparing AFB_1 adsorption values in percentage (at pH7) with some characteristics of bentonites (swell index, sodium and

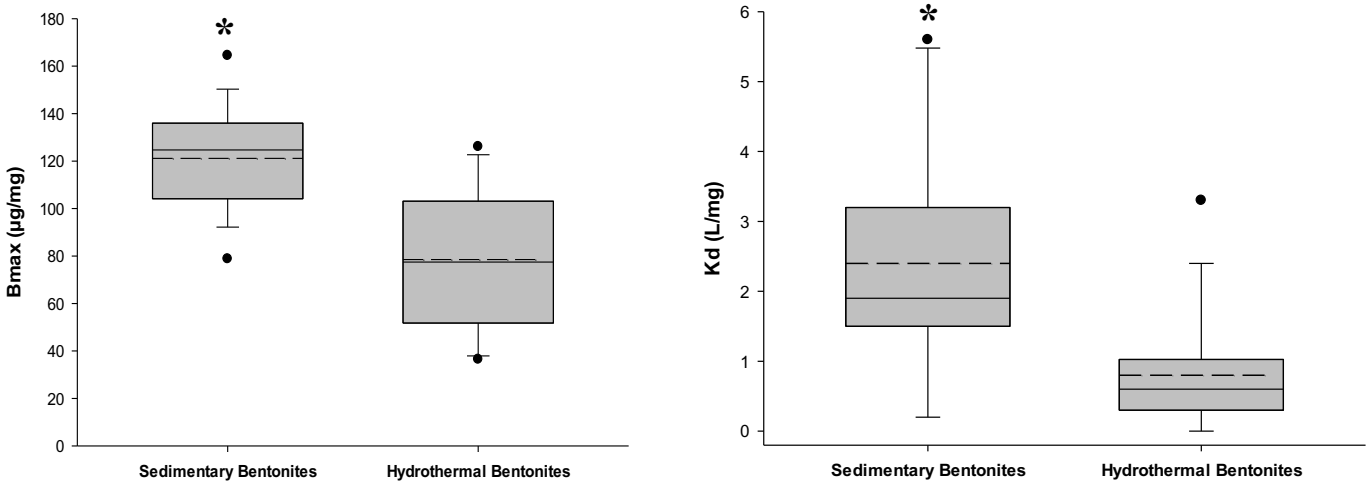

Fig. 5. Distribution of B_{max} and K_d values measured for sedimentary and hydrothermal bentonites by adsorption isotherms. The mean and median values are marked by dotted and black lines, respectively. The superscript * in each box plot indicates statistical difference between the two groups of bentonites ($p_{t\text{-}test} < 0.001$).

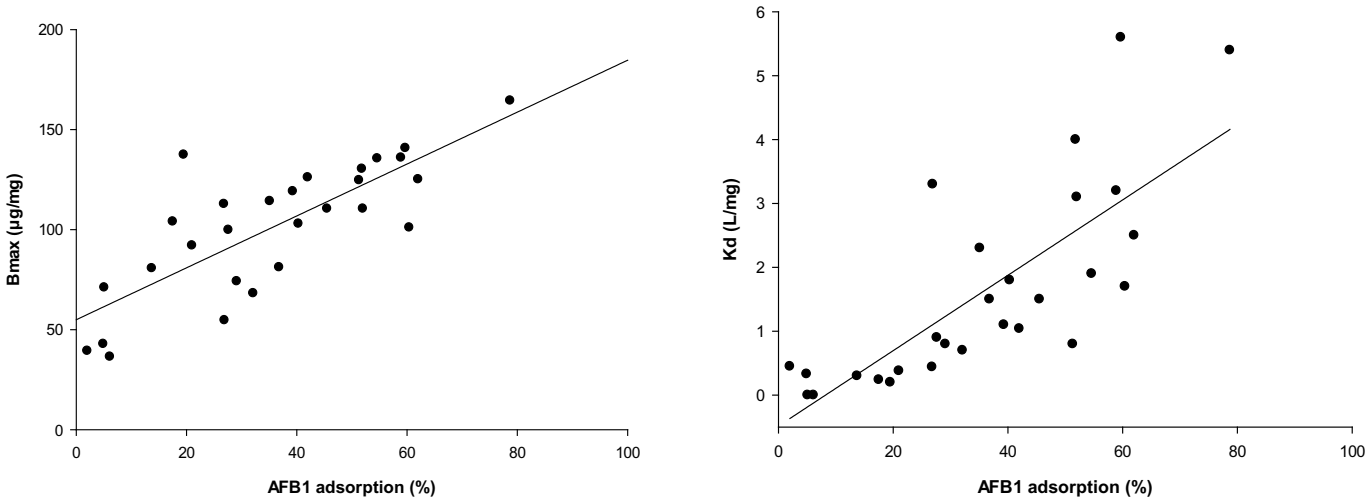

Fig. 6. Regression lines between B_{max} and K_d *vs* AFB_1 adsorption values measured for all samples. B_{max} and K_d values were calculated by adsorption isotherms, while AFB_1 adsorption values as percentage were obtained by preliminary adsorption tests.

Table 4
Adsorption values obtained at pH7, desorption values by methanol, and chemisorptions index values calculated for sedimentary (S1-S15) and hydrothermal (H1-H14) bentonites. Values are means ± standard deviations of triplicate independent experiments.

Sample code	Adsorption (%)	Desorption (%)	C_α
S4	93.30 ± 0.01	62 ± 2	0.35 ± 0.02
S13	93.1 ± 0.3	51.7 ± 1.7	0.46 ± 0.02
S5	98.5 ± 0.5	46 ± 2	0.53 ± 0.02
S2	88.4 ± 0.7	44 ± 3	0.55 ± 0.03
S9	98.6 ± 0.5	42.0 ± 0.9	0.57 ± 0.01
S6	97.0 ± 0.9	38.7 ± 0.8	0.59 ± 0.00
S10	98.8 ± 0.1	39.6 ± 1.3	0.60 ± 0.01
S15	99.0 ± 0.2	33.5 ± 0.8	0.66 ± 0.10
S11	97.7 ± 0.1	25.0 ± 1.0	0.73 ± 0.01
S1	98.1 ± 0.2	17.7 ± 1.2	0.81 ± 0.01
S8	98 ± 3	16.4 ± 0.5	0.82 ± 0.03
S14	98.2 ± 0.1	15 ± 5	0.83 ± 0.05
S6	97.9 ± 0.1	9.6 ± 1.5	0.89 ± 0.01
S3	97.2 ± 0.2	7.1 ± 1.7	0.90 ± 0.01
S12	97.1 ± 0.6	7.4 ± 0.3	0.90 ± 0.01
H3	91.1 ± 0.3	77.6 ± 1.9	0.20 ± 0.02
H6	76.8 ± 1.0	62 ± 6	0.29 ± 0.02
H1	82.4 ± 0.9	64 ± 3	0.29 ± 0.04
H11	93.9 ± 0.9	68 ± 3	0.33 ± 0.06
H5	98.0 ± 0.2	62.1 ± 0.9	0.37 ± 0.01
H7	98.3 ± 0.1	59.6 ± 0.7	0.40 ± 0.01
H10	92.4 ± 0.1	53 ± 3	0.44 ± 0.03
H12	93.7 ± 0.4	48 ± 3	0.48 ± 0.03
H9	95.4 ± 0.4	47.2 ± 0.7	0.50 ± 0.00
H13	97.7 ± 0.1	36 ± 5	0.59 ± 0.04
H14	98.0 ± 0.4	36 ± 3	0.61 ± 0.04
H2	98.5 ± 0.2	13.2 ± 0.9	0.81 ± 0.01
H4	99.70 ± 0.01	10.4 ± 0.3	0.85 ± 0.00
H8	94.7 ± 1.1	8.4 ± 0.5	0.86 ± 0.01

magnesium contents, and d001-value) (Fig. 9). These findings show that AFB_1 adsorption by bentonites is favored by the presence of sodium as major exchangeable ion in the dominant mineral (smectite), and then by their capacity to swell in the presence of water, being sodium content and swelling properties positively correlated. As a consequence of sodium abundance of a bentonite sample in favoring AFB_1 adsorption, toxin adsorptions (Ads % and B_{max} values) were negatively correlated to d001-values ($p < 0.001$) (Table 5). Indeed, sodium content negatively correlated to d001-values ($p < 0.0001$, $CC = -0.821$). Interestingly, a significant negative correlation ($p < 0.001$) was found between the results of adsorption studies and magnesium content (Table 5). Finally,

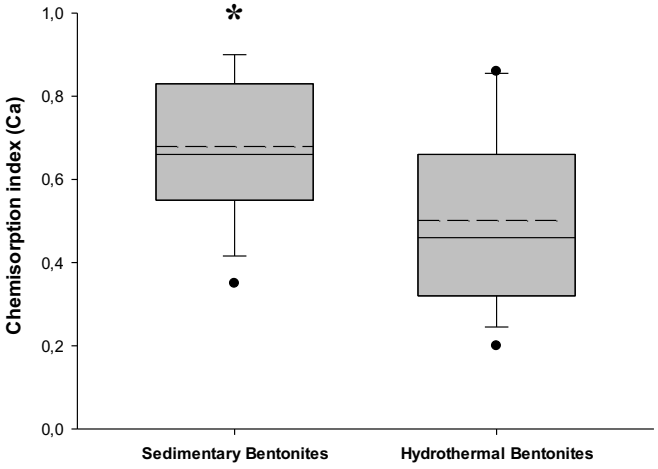

Fig. 7. Distribution of chemisorption index values (Cα) measured for sedimentary and hydrothermal bentonites. The mean and median values are marked by dotted and black lines, respectively. The superscript * in each box plot indicates statistical difference between the two groups of bentonites ($p_{t\text{-}test} < 0.05$).

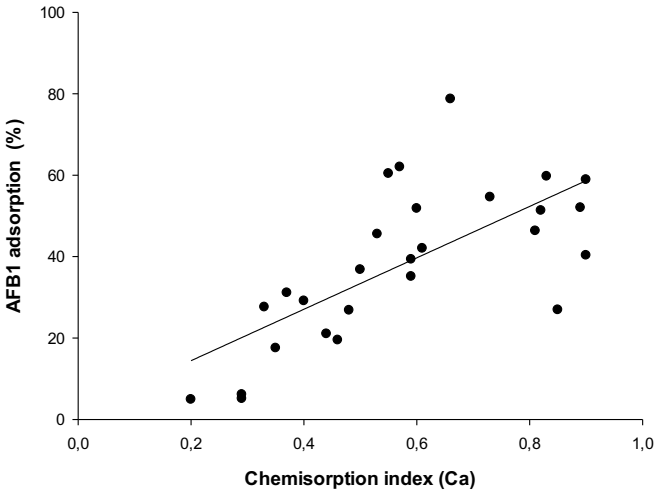

Fig. 8. Regression line of AFB_1 adsorption values *vs* chemisorption index values (Cα) measured for all samples.

Table 5
Pearson's correlations between AFB_1 adsorption values expressed as percentage (measured at different pH values) or B_{max} (measured by adsorption isotherms) and physico-chemical parameters (swell index, d001-value, Na, Mg, Ca and Fe contents, and CEC). Pearson correlation coefficient (CC) and p-value index were used to establish the goodness of correlations.

	AFB_1 adsorption (%)				B_{max}	
	pH 7		pH 3			
	CC	p-value	CC	p-value	CC	p-value
Swell	**0.669**	**< 0.001**	**0.710**	**< 0.001**	**0.712**	**< 0.001**
d001	**-0.630**	**< 0.001**	**-0.741**	**< 0.001**	**-0.767**	**< 0.001**
CEC	-0.363	0.053	-0.267	0.162	-0.269	0.159
Na	**0.485**	**< 0.001**	**0.481**	**< 0.001**	**0.551**	**0.002**
Mg	**-0.534**	**< 0.001**	**-0.533**	**< 0.001**	**-0.609**	**< 0.001**
Ca	-0.344	0.068	-0.322	0.089	**-0.457**	**0.013**
Fe	-0.138	0.476	-0.015	0.940	0.058	0.765

Values in bold are statistically significant.

also calcium content of bentonites negatively correlated to B_{max} values ($CC = -0.457$, $p = 0.0013$), although no significant correlation was found between calcium content and adsorption values in percentage. No correlation was found between all AFB_1 adsorption results and iron content or CEC. Looking at some single bentonites belonging to the two groups of samples, further observations can be done. Within the group of sedimentary bentonites, only one sample (S5) was identified as a calcium-smectite containing bentonite. It showed high contents of calcium, iron and magnesium, and poor swelling properties (Tables 1A-2A). Interestingly, it had good AFB_1 adsorption efficacy, but poor ability in retaining the adsorbed fraction of the toxin when extracted by methanol (Table 4). Within the group of sedimentary bentonites, samples S4 and S13 which contained mainly smectites with a mixed sodium/calcium assemblage and a high content of iron showed poor swelling properties and, at the same time, the lowest values for AFB_1 adsorption (Figs. 2 and 4), affinity ($K_d < 1$ L/mg) (Table3), and C_α (Table 4). On the other side, within the group of hydrothermal bentonites, some sodium/calcium smectites that showed good swelling properties and at the same time high content of iron (namely, samples H8, H9, H12, H13 and H14) were found as the best performing materials of the group for toxin adsorption. These "semi-sodic" smectites were not excluded from the correlation analyses and may explain the apparent overlapping of adsorption results for the two groups (Figs. 2 and 4). The best aflatoxin adsorbing samples in the hydrothermal (calcium-smectite) group (i.e., H12, H13 and H14) were identified as sodic-calcic mixed smectites. On the other hand, in the group of sedimentary sodium-bentonites, the samples with a mixed sodic-calcic

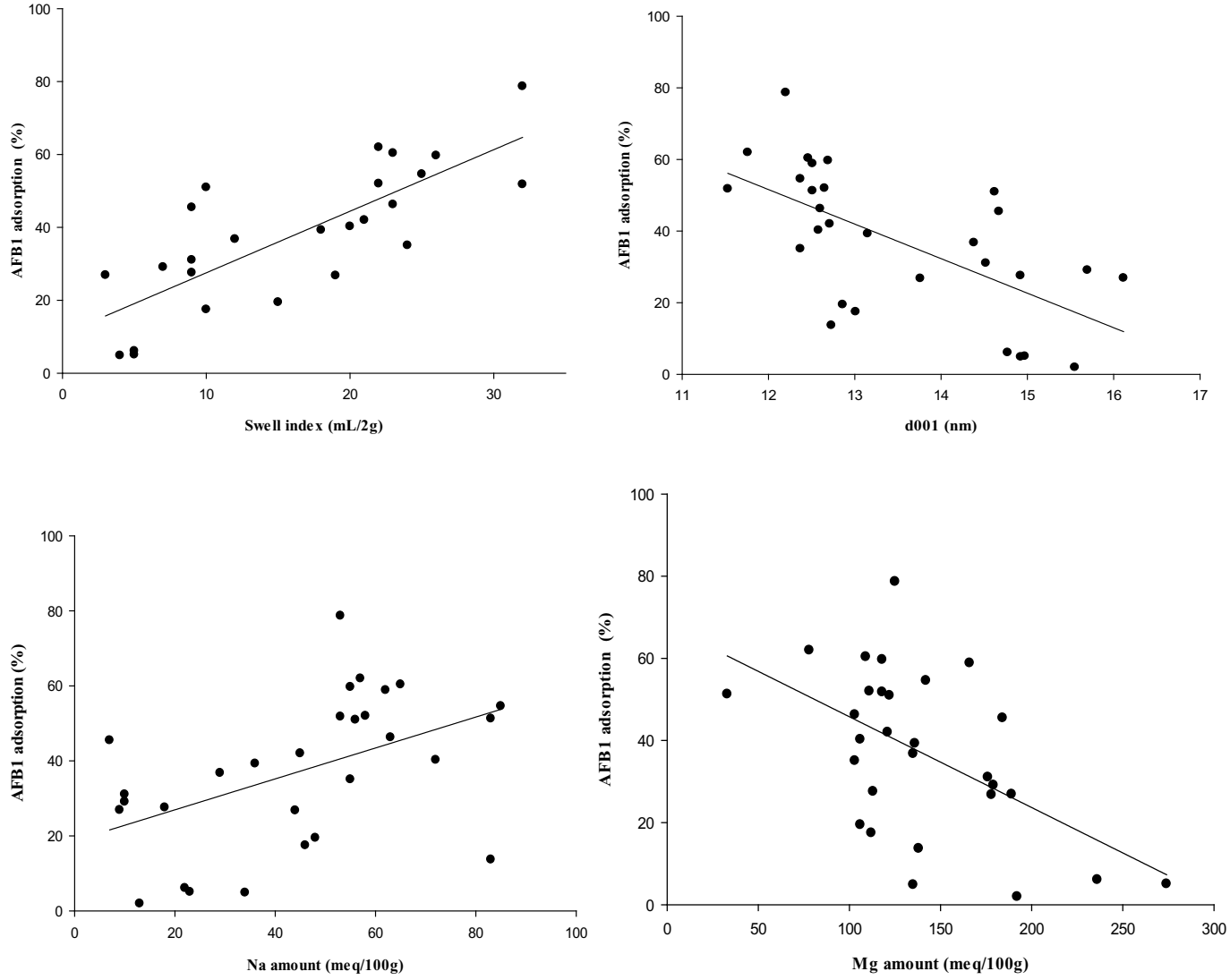

Fig. 9. Regression lines of AFB_1 adsorption values *vs* physico-chemical parameters (swell index, Na content, Mg content and d001-value) measured for all samples.

structure (S4 and S13) were the less performing adsorbing minerals.

It is well known that sodium is the dominant ion in the sedimentary bentonites and calcium is the dominant ion in the hydrothermal bentonites, which exhibit markedly different properties and thus uses. The terms swelling bentonites and nonswelling bentonites are largely used as synonymous of sodium bentonites and calcium bentonites. When mixed with water, swelling bentonites exhibit a greater degree of dispersion and better plastic and rheological properties than nonswelling bentonites (Inglethorpe et al., 1993). This was confirmed by our study. In addition, we showed that sedimentary and hydrothermal bentonites differed also in their ability in acting as AFB_1 binders, being sedimentary bentonites more performing than hydrothermal ones. More, our findings suggest that the different behavior of sedimentary and hydrothermal bentonites in sequestering AFB_1 and in retaining the adsorbed fraction of the toxin may be related to some "intrinsic" properties of their smectites. It seems that the amount of AFB_1 adsorbed by the smectite minerals in the samples is strongly influenced by the dominant exchangeable cations. The monovalent cations as sodium offered better conditions for AFB_1 adsorption than calcium in the smectites. In addition to calcium, magnesium content seems to influence negatively AFB_1 uptake. The presence of iron in the octahedral sheet did not enhance AFB_1 adsorption, except maybe for some hydrothermal samples containing a mixed sodium/calcium assemblage. Taking into account the little content of subordinate minerals in bentonite samples, it can be assumed that most of these cations were in the dominant mineral, i.e. smectites. Rheological properties of smectites such as swell index seem to enhance toxin adsorption as well.

These findings are in contrast with previous works (Grant and Phillips, 1998; Dixon et al., 2008; Deng et al., 2012) showing that calcium-bentonites or bentonite containing iron and magnesium in the structure are in general better AFB_1 binders than sodium-bentonites. However, the study of Kannewischer et al. (2006) testing a large number of smectites samples (20) mined from different locations in the United States and Mexico showed that calcium ion content of their smectite samples did not have a distinct influence on AFB_1 adsorption. Similarly, other cations present in their smectite samples seemed to have no effect on the sorption ability of the "as received" smectites. Due to the complexity of the interactions and factors that can be involved in the aflatoxin adsorption by smectites, further research is needed to determine the proper adsorption mechanisms.

4. Conclusions

In the effort to identify the most critical mineralogical, chemical, and physical properties that affect the adsorption capacity and selectivity of bentonites for AFB_1, bentonite samples from different sources around the world and different geological origin were evaluated. Twenty-nine samples behaving like smectites were chosen to focus on characterization as AFB_1 adsorbents. Natural samples ("as received") were divided into two main groups, i.e. hydrothermal ($n = 14$) and sedimentary ($n = 15$) bentonites depending on their geological origin. The characterization study showed that all samples contained mainly smectite (montmorillonite), although they differed significantly in some physico-chemical properties. All samples had a large smectite content, a moderate CEC value between 60-116 cmol/kg, the presence of iron in the octahedral sheet of the smectite, a small organic matter content, a near-neutral pH, and a fine and uniform particle size ($< 45\mu m$). They differed substantially in their sodium, calcium and magnesium contents, and in the swelling properties. Several *in vitro* adsorption studies were performed to assess their ability in adsorbing AFB_1, and in retaining the fraction of the adsorbed toxin. Single-concentration adsorption studies were performed in buffer solutions at physiological pH values, using a very low adsorbent concentration (0.001% w/v) and a high toxin amount (1 μg/mL). Isothermal adsorption experiments were included to determine the main features of the adsorption process (maximum adsorption capacity and adsorption affinity), using a very low adsorbent concentration (0.005% w/v) to assure the saturation of the binders with the adsorbate. In addition, desorption studies by methanolic extraction were carried out to determine the strength of the binding. Although, all samples showed most properties required to have "good" AFB_1-adsorbing bentonites, they differed in their ability in adsorbing the toxin. Five-fold differences both in adsorption, based on the Langmuir equation, and in desorption of the toxin were observed. For the first time, a correlation between geological origin of smectites and AFB_1 adsorption capacity was found. In particular, sedimentary smectites were significantly more effective than hydrothermal smectites in adsorbing the toxin at different pH values. The high adsorption capacity and adsorption affinity of sedimentary smectites towards AFB_1 was confirmed by adsorption isotherm studies. Most of sedimentary smectites showed B_{max} values higher than 100 μg/mg (0.32 mol/kg) and K_d values higher than 1.0 L/mg (312 500 L/mol), indicating high adsorption capacity and affinity for the binding of the toxin. Interestingly, the extent of AFB_1-adsorption by smectites was negatively and linearly correlated to the extent of desorption, and sedimentary smectites were significantly more effective than hydrothermal smectites in keeping bound the adsorbed fraction. Further correlation studies using the Pearson statistical method showed that AFB_1 adsorption of smectites correlated positively with sodium content and swell index, but negatively with basal spacing (d001-value), magnesium content and calcium content. The experiments performed in this study cannot fully explain why the two groups of smectites differ substantially in adsorbing the toxin, and it is still difficult to depict a strong relationship among the physico-chemical properties of these AFB_1-adsorbing minerals and the amounts of adsorbed/desorbed toxin. It can be supposed that some of "intrinsic" properties of smectites belonging to different geological groups may affect AFB_1 adsorption. A "cryptic variation" in these physico-chemical properties of smectites may be a cause of the different behavior of smectites in sequestering the mycotoxin. More samples mined from different locations and belonging to these geological groups need to be investigated. In addition, more intensive investigations of individual structural properties are required.

Acknowledgements

This research was financially supported by the research agreement between CNR-ISPA and Laviosa Chimica Mineraria SpA (CNR Prot. No. 3123 on 27/06/2016); and by the European Union's Horizon2020 Research and innovation programme under Grant Agreement No.678781 (MycoKey).

References

Afriyie-Gyawu, E., Ankrah, N.A., Huebner, H., Ofosuhene, M., Kumi, J., Johnson, N., Tang, L., Xu, L., Jolly, P., Ellis, P., Ofori-Adjei, D., Williams, J.H., Wang, J.S., Phillips, T.D., 2008a. NovaSil clay intervention in Ghanaians at high risk for aflatoxicosis, part I: study design and clinical outcomes. Food Addit. Contam. 25 (1), 76–87.

Afriyie-Gyawu, E., Wang, Z., Ankrah, N.A., Xu, L., Johnson, N.M., Tang, L., Guan, H., Huebner, H.J., Jolly, P.E., Ellis, W.O., Taylor, R., Brattin, B., Ofori-Adjei, D., Williams, J.H., Wang, J.S., Phillips, T.D., 2008b. NovaSil clay does not affect the concentrations of vitamins A and E and nutrient minerals in serum samples from Ghanaians at high risk for aflatoxicosis. Food Addit. Contam. Part A 25 (7), 872–884.

Alshameria, A., Xi, Y., Zhu, R., Ma, L., 2018. Adsorption of ammonium by different natural clay minerals: Characterization, kinetics and adsorption isotherms. Appl.Clay Sci. 159, 83–93.

Altaner, S.P., Ylagan, R.F., 1997. Comparison of structural models of mixed-layer illite/smectite and reaction mechanisms of smectite illitization. Clays Clay Miner. 45, 517–533.

AOAC Official Method of Analysis, 2000. Preparation of Standards for Aflatoxins (49.2.02), AOAC Official Method 970.44. Chapter 49. pp. 3–4.

ASTM D2216-10, 2010. Standard Test Methods for Laboratory Determination of Water (Moisture) Content of Soil and Rock by Mass. ASTM International, West Conshohocken, PA.

ASTM D4373-14, 2014. Standard Test Method for Rapid Determination of Carbonate Content of Soils. ASTM International, West Conshohocken, PA.

ASTM D4972-18, 2018. Standard Test Methods for pH of Soils. ASTM International, West Conshohocken, PA.

ASTM D5890 Standard, 2011. Standard test method for swell index of clay mineral component of geosynthetic clay liners. ASTM International, West Conshohocken, PA.
Avantaggiato, G., Visconti, A., 2009. Mycotoxin Issues in farm animals and strategies to reduce mycotoxins in animal feeds. In: Wiseman, J., Garnsworthy, P. (Eds.), Recent Advances in Animal Nutrition-2009. Nottingham University Press, Nottingham, 978-1-907284-65-6, pp. 149–189.
Avantaggiato, G., Greco, D., Damascelli, A., Solfrizzo, M., Visconti, A., 2014. Assessment of multi-mycotoxin adsorption efficacy of Grape Pomace. J. Agric. Food Chem. 62 (2), 497–507.
Barrientos-Velázquez, A.L., Marroquin-Cardona, A., Liu, L., Phillips, T., Deng, Y., 2016. Influence of layer charge origin and layer charge density of smectites on their aflatoxin adsorption. Ana. Appl. Clay Sci. 132 (133), 281–289.
Bergaya, F., Lagaly, G., 2013. General introduction: clays, clay minerals, and clay science. In: Bergaya, F., Lagaly, G. (Eds.), Handbook of Clay Science. Elsevier, Amsterdam, pp. 1–19.
C837-09, A.S.T.M., 2014. Standard Test Method for Methylene Blue Index of Clay. ASTM International, West Conshohocken, PA.
Carretero, M.I., Lagaly, G., 2007. Clays and health: An introduction. Appl. Clay Sci. 36, 1–3.
Charturvedi, V.B., Singh, K.S., Agnihotri, A.K., 2002. In vitro aflatoxin adsorption capacity of some indigenous aflatoxin sorbent. Indian J. Anim. Sci. 72 (3), 257–260.
Christidis, G., Huff, D.H., 2009. Geologic aspects and genesis of bentonites. Elements 5, 93–98.
Commission Implementing Regulation (EU) No 1060/2013 of 29 October 2013 concerning the authorisation of bentonite as a feed additive for all animal species, OJ L 289, 31.10.2013, 33.
Commission Regulation (EU) No 380/2012 of 3 May 2012 amending Annex II to Regulation (EC) No 1333/2008 of the European Parliament and of the Council as regards the conditions of use and the use levels for aluminium-containing food additives. OJ L 119, 14
Deng, Y., Liu, L., Barrientos Velazquez, A.L., Dixon, J.B., 2012. The determinative role of the exchange cation and layer-charge density of smectite on aflatoxin adsorption. Clay Clay Miner. 60, 374–386.
Desheng, Q., Fan, L., Yanhu, Y., Niya, Z., 2005. Adsorption of aflatoxin B-1 on montmorillonite. Poult. Sci. 84 (6), 959–961.
Díaza, E., Voisina, L., Krachta, W., Montenegro, V., 2018. Using advanced mineral characterisation techniques to estimate grinding media consumption at laboratory scale. Miner. Eng. 121, 180–188.
Dixon, J.B., Kannewischer, I., Tenorio Arvide, M.G., Barrientos Velazquez, A.L., 2008. Aflatoxin sequestration in animal feeds by quality-labeled smectite clays: An introductory plan. Appl. Clay Sci. 40, 201–208.
EFSA, 2004. Opinion of the Scientific Panel on Contaminants in the Food Chain on a request from the commission related to aflatoxin B_1 as undesirable substance in animal feed. EFSA J. 39, 1–27.
Foo, K.Y., Hameed, B.H., 2010. Insights into the modeling of adsorption isotherm systems. Chem Eng J 156, 2–10.
Galan, E., Castillo, A., 1984. Sepiolite-Palygorskite in Spanish Tertiary Basins; genetical patterns in continental environments. In: Singer, A., Galan, E. (Eds.), Palygorskite-Sepiolite Occurrences, Genesis and Uses, Developments in Sedimentology, pp. 87–124.
Grant, P.G., Phillips, T.D., 1998. Isothermal adsorption of aflatoxin B_1 on HSCAS clay. J. Agric. Food Chem. 46, 599–605.
Greco, D., D'Ascanio, V., Santovito, E., Logrieco, A.F., Avantaggiato, G., 2018. Comparative efficacy of agricultural by-products in sequestering mycotoxins. J. Sci. Food Agric. 99, 1623–1634.
Grim, R.E., Güven, N., 1978. Bentonites, Geology, Mineralogy, Properties and Uses, Development in Sedimentology. 24 Elsevier, Amsterdam.
Inglethorpe, S.D.J., Morgan, D.J., Highley, D.E., Bloodworth, A.J., 1993. Industrial Minerals Laboratory Manual BENTONITE. BGS Technical Report WG/93/20.
Jaynes, W.F., Zartman, R.E., 2011. Influence of soluble feed proteins and clay additive charge density on aflatoxin binding in ingested feeds. In: Guevara-Gonzalez, R. (Ed.), Aflatoxins Biochemistry and Molecular Biology. InTech.
JECFA, 2018. Safety evaluation of certain contaminants in food. In: WHO Food Additives Series, No. 74; FAO JECFA Monographs 19 bis, ISBN 978-92-4-166074-7.
Kannewischer, I., Tenorio Arvide, M.G., White, G.N., Dixon, J.B., 2006. Smectite clays as adsorbents of aflatoxin B_1: initial steps. Clay Sci., Japan 12 (Supplement 2), 199–204.
Li, Y., Tian, G., Dong, G., Bai, S., Han, X., Liang, J., Meng, J., Zhang, H., 2018. Research progress on the raw and modified montmorillonites as adsorbents for mycotoxins: A review. Appl. Clay Sci. 163, 299–311.
Magnoli, A.P., Cabaglieri, L.R., Magnoli, C.E., Monge, J.C., Miazzo, R.D., Peralta, M.F., Salvano, M.A., Rosa, C.A.R., Dalcero, A.M., Chiacchiera, S.M., 2008. Bentonite performance on boiler chickens fed with diets containing natural levels of aflatoxin B_1. Rev. Bras. Med. Vet 30 (1), 55–60.
Marquez, R.N., Hernandez, I.T.D., 1995. Aflatoxin adsorbent capacity of two Mexican aluminosilicates in experimentally contaminated chick diets. Food Addit. Contam. 431–433.
Marroquın-Cardona, A., Deng, Y., Taylor, J.F., Hallmark, C.T., Johnson, N.M., Phillips, T.D., 2009. In vitro and in vivo characterization of mycotoxin-binding additives used for animal feeds in Mexico. Food Addit. Contam. 26 (5), 733–743.
Masimango, N., Remacle, J., Ramaut, J., 1978. The role of adsorption in the elimination of aflatoxin B_1 from contaminated media. Eur. J. Appl. Micorbiol. Biotechnol. 6 (1), 101–105.
Masimango, N., Remacle, J., Ramaut, J., 1979. Elimination of aflatoxin B_1 from contaminated media by swollen clays. Ann. Nutr. Aliment. 33 (1), 137–147.
Miyoshi, Y., Ishibashi, J., Faure, K., Maeto, K., Matsukura, S., Omura, A., Shimada, K., Sato, H., Sakamoto, T., Uehara, S., Chiba, H., Yamanaka, T., 2013. Mg-rich clay mineral formation associated with marine shallow-water hydrothermal activity in an arc volcanic caldera setting. Chem. Geol. 355, 28–44.
Moore, D., Reynolds, R., 1989. X-ray Diffraction and the Identification and Analysis of Clay Minerals. Oxford University Press, Oxford, UK.
Motulsky, H., Ransnas, L.A., 1987. Fitting curves to data using nonlinear regression: a practical and nonmathematical review. FASEB J. 1 (5), 365–374.
Mulder, I., Barrientos Velazquez, A.L., Tenorio Arvide, M.G., White, G.N., Dixon, J.B., 2008. Smectite clay sequestration of aflatoxin B1: mineral dispersivity and morphology. Clay Clay Miner. 56, 559–571.
Nahm, K.H., 1995. Prevention of aflatoxicosis by addition of antioxidants and hydrated sodium calcium aluminosilicates to the diet of young chicks. Nippon Kakin Gakkaishi 32 (2), 117–127.
Pharmacopoeia, U.S., 2005. The official compendia of standards. USP 28 NF 23. Twinbrook Parkway: USP Convention Inc, pp. 2961.
Phillips, T.D., Kubena, L.F., Harvey, R.B., Taylor, D.R., Heidelbaugh, N.D., 1988. Hydrated sodium calcium aluminosilicate: a high affinity sorbent for aflatoxin. Poult. Sci. 67, 243–247.
Phillips, T.D., Grant, P.G., Sarr, A.B., 1995. Selective chemisorption and detoxication of aflatoxins by phyllosilicate clay. Nat. Toxins 3, 204–213.
Phillips, T.D., Afriyie-Gyawu, E., Williams, J., Huebner, H., Ankrah, N.A., Ofori-Adjei, D., Jolly, P., Johnson, N., Taylor, J., Marroquin-Cardona, A., Xu, L., Tang, L., Wang, J.S., 2008. Reducing human exposure to aflatoxin through the use of clay: a review. Food Addit. Contam. 25, 134–145.
Ramos, A.J., Hernández, E., 1996. In vitro aflatoxin adsorption by means of a montmorillonite silicate. A study of adsorption isotherms. Anim. Feed Sci. Technol. 62, 263–269.
Sinha, R., Raymahashay, B.C., 2004. Evaporite mineralogy and geochemical evolution of the Sambhar Salt Lake, Rajasthan, India. Sediment. Geol. 166, 59–71.
Taylor, R.K., 1985. Cation exchange in clays and mudrocks by methylene blue. J. Chem. Technol. Biotechnol. Chem. Technol. 35 (4), 195–207.
Tenorio Arvide, M.G., Mulder, I., Barrientos Velazquez, A.L., Dixon, J.B., 2008. Smectite clay adsorption of aflatoxin versus octahedral composition, as indicated by FTIR. Clay Clay Miner. 56, 571–578.
Vekiru, E., Fruhauf, S., Sahin, M., Ottner, F., Schatzmayr, G., Krska, R., 2007. Investigation of various adsorbents for their ability to bind Aflatoxin B_1. Mycotoxin Res. 23 (1), 27–33.
Vekiru, E., Fruhauf, S., Rodrigues, I., Ottner, F., Krska, R., Schatzmayr, G., Ledoux, D., Rottinghaus, G., Bermudez, A., 2015. In vitro binding assessment and in vivo efficacy of several adsorbents against aflatoxin B1. World Mycotoxin J. 8 (4), 477–488.
Vila-Donat, P., Marìn, S., Sanchis, V., Ramos, A.J., 2018. A review of the mycotoxin adsorbing agents, with an emphasis on their multi-binding capacity, for animal feed decontamination. Food Chem. Toxicol. 114, 246–259.
Wang, J.S., Luo, H., Billam, M., Wang, Z., Guan, H., Tang, L., Goldston, T., Afriyie-Gyawu, E., Lovett, C., Griswold, J., Brattin, B., Taylor, R.J., Huebner, H.J., Phillips, T.D., 2005. Short term safety evaluation of processed calcium montmorillonite clay (NovaSil) in humans. Food Addit. Contam. 22, 270–279.
Wang, P., Afriyie-Ggawu, E., Tang, Y., Johnson, N.M., Xu, L., Tang, L., Huebner, H.J., Ankrah, N.A., Ofori-Adjei, D., Ellis, W., Jolly, P.E., Williams, J.H., Wang, J.S., Phillips, T.D., 2008. NovaSil clay intervention in Ghanaians at high risk for aflatoxicosis: II. Reduction in biomarkers of aflatoxin in blood and urine. Food Addit. Contam. Part A 25 (5), 622–634.
WHO (World Health Organization), 2005. Bentonite, kaolin, and selected clay minerals. World health organization, international programme on chemical safety vol. World Health Organization, Geneva, Switzerland, pp. 231.